X-620-73-82

PREPRINT

NASA TM X- 66230

# MARTIAN TIDAL PRESSURE AND WIND FIELDS OBTAINED FROM THE MARINER 9 INFRARED SPECTROSCOPY EXPERIMENT

MARCH 1973



GSFC

GODDARD SPACE FLIGHT CENTER

GREENBELT, MARYLAND

X-620-73-82

# MARTIAN TIDAL PRESSURE AND WIND FIELDS OBTAINED FROM THE MARINER 9 INFRARED SPECTROSCOPY EXPERIMENT

Joseph A. Pirraglia

Barney J. Conrath

March 1973

Goddard Space Flight Center

Greenbelt, Maryland

CONTENTS

# MARTIAN TIDAL PRESSURE AND WIND FIELDS OBTAINED FROM THE MARINER 9 INFRARED SPECTROSCOPY EXPERIMENT

by

Joseph A. Pirraglia*

Barney J. Conrath

## ABSTRACT

Using temperature fields derived from the Mariner 9 infrared spectroscopy experiment, the Martian atmospheric tidal pressure and wind fields are calculated. Temperature as a function of local time, latitude, and atmospheric pressure level is obtained by secular and longitudinal averaging of the data. The resulting temperature field is approximated by a spherical harmonic expansion, retaining one symmetric and one asymmetric term each for wavenumber zero and wavenumber one. Vertical averaging of the linearized momentum and continuity equations results in an inhomogeneous tidal equation for surface pressure fluctuations with the driving function related to the temperature field through the geopotential function and the hydrostatic equation. Solutions of the tidal equation show a diurnal fractional pressure amplitude approximately equal to one half of the vertically averaged diurnal fractional temperature amplitude. These results indicate

* NRC-NASA Resident Research Associate

that a diurnal pressure fluctuation of 6-7% existed during the planet-wide dust storm of 1971-72 as well as during its subsequent decay. The calculated tidal pressure fields, along with the temperature fields, yield tidal wind velocities of the order of 10 meters per second near the lower boundary, assumed to be friction free in the model. Dynamic heating accounts for 3-4°K of the diurnal amplitude of the vertically averaged temperature.

# MARTIAN TIDAL PRESSURE AND WIND FIELDS OBTAINED FROM THE MARINER 9 INFRARED SPECTROSCOPY EXPERIMENT

## INTRODUCTION

Temperature profiles obtained from measurements in the 667 $cm^{-1}$ $CO_2$ band by the infrared interferometer spectrometer experiment on Mariner 9 have been used to construct semi-global temperature fields for the Martian atmosphere in the form of longitudinal averaged temperatures at various pressure levels given as functions of latitude and local time. During the great dust storm of 1971, a strong local time dependence of the temperature throughout the full depth of the lower atmosphere was observed. Using a dynamical model which assumed a constant surface pressure, the temperatures fields have been employed to estimate the Martian winds which existed during the dust storm (Hanel, et al, 1972). However, the temperature data suggest an appreciable tidal motion forced by diurnal heating. The object of the present paper is to investigate the tidal surface pressure variations and associated wind fields again using the observed temperatures as input data. In addition to the purely tidal motion, the investigation includes local time averaged fields, i.e., those fields which are symmetric with respect to the polar axis.

## SURFACE PRESSURE TIDAL EQUATION

The set of equations which describes the motion of the atmosphere is simplified when the temperature, rather than the heat input, is used as the known

driving mechanism. The heating required to be consistent with the observed temperatures may then be calculated. Using the perfect gas law and the hydrostatic approximation, the equations of motion in $\sigma$-coordinates (Phillips, 1957) can be written

$$\frac{\partial \mathbf{v}}{\partial t} + \mathbf{v}\cdot\nabla\mathbf{v} + \dot{\sigma}\frac{\partial \dot{\sigma}}{\partial \sigma} + \frac{RT}{p_s}\nabla p_s + \nabla\Phi + f\mathbf{k}\times\mathbf{v} = \mathbf{F} \tag{1}$$

$$p_s\dot{\sigma} = -\int_1^{\sigma} \nabla\cdot(p_s\mathbf{v})\,d\sigma - (\sigma - 1)\frac{\partial p_s}{\partial t} \tag{2}$$

$$\Phi = -R\int_1^{\sigma} \frac{T}{\sigma'}\,d\sigma' + \Phi_s \tag{3}$$

The following notation is employed:

$\theta$, colatitude;

$\phi$, longitude measured from west to east;

$\Omega$, rotational angular velocity;

$t$, time;

$R$, $CO_2$ gas constant;

$p_s$, surface pressure;

$p$, pressure;

$\sigma$, pressure ratio, $p/p_s$;

$\mathbf{k}$, unit vector in radial direction;

$\nabla$, horizontal gradient operator on constant $\sigma$ surface;

$\mathbf{v}$, horizontal velocity on $\sigma$-surface;

$T$, temperature;

$\dot{\sigma}$, vertical velocity in $\sigma$-coordinates;

$\mathbf{F}$, frictional forces;

$f$, coriolis parameter, $2\Omega \sin\theta$;

$\Phi_s$, the geopotential on surface $\sigma = 1$.

Assume that the temperature may be expressed in terms of $T_0$, a temperature field associated with a static atmosphere, and $T_1$, a temperature associated with atmospheric motion, in the form

$$T = T_0 + \epsilon T_1,$$

where $\epsilon$ is a small quantity. Expanding the variables $\mathbf{v}$, $\dot{\sigma}$, $p_s$ and $\Phi$ in terms of $\epsilon$ about the static case, designating the static terms by subscript 0 and first order terms by subscript 1, and using the boundary condition $\dot{\sigma} = 0$ at $\sigma = 0$ and $\sigma = 1$, the first order equations are

$$\frac{\partial \mathbf{v}_1}{\partial t} + f\mathbf{k} \times \mathbf{v}_1 + \frac{RT_0}{p_{s0}} \nabla p_{s1} + \left( T_1 - \frac{T_0 p_s}{p_{s0}} \right) \frac{\nabla p_{s0}}{p_{s0}} + \nabla \Phi_1 = \mathbf{F} \tag{4}$$

$$\frac{\partial p_{s1}}{\partial t} + p_{s0} \int_0^1 \nabla \cdot \mathbf{v}_1 \, d\sigma + \nabla p_{s0} \cdot \int_0^1 \mathbf{v}_1 \, d\sigma = 0 \tag{5}$$

$$\Phi_1 = -R \int_1^\sigma \frac{T_1}{\sigma'} \, d\sigma'. \tag{6}$$

Neglecting orographic effects, $p_{s0}$ is constant on the surface $\sigma = 1$ and the fourth term of (4) and the third term of (5) can be dropped. For a static case

in which $p_{s0}$ is not constant, the terms could be dropped and later used to assess the validity of neglecting orographic effects. Only the first order equations will be considered.

Averaging (4) and (6) over $\sigma$ from 0 to 1 and denoting $\sigma$-averaged quantities by an over-bar, the equations of motion for the vertically averaged velocity and surface pressure are

$$\frac{\partial \bar{\mathbf{v}}_1}{\partial t} + f\mathbf{k} \times \bar{\mathbf{v}}_1 + \frac{R\bar{T}_0}{p_{s0}} \nabla p_{s1} + \nabla \Phi_1 = \bar{\mathbf{F}} \tag{7}$$

$$\frac{\partial p_{s1}}{\partial t} + p_{s0} \nabla \cdot \bar{\mathbf{v}}_1 = 0. \tag{8}$$

$$\bar{\Phi}_1 = R\bar{T}_1. \tag{9}$$

The friction term $\mathbf{F}$ depends upon the internal velocity shearing stress and the shearing stress at the boundary. The concern here is with the wind regime outside the surface boundary layer and with the surface pressure variations. Since the motion is forced, the bulk of the flow and the resulting surface pressure should not be greatly affected by the surface drag except possibly for the axially symmetric flow in which friction causes a small meridional component that allows a latitudinal redistribution of the atmosphere. With these observations in mind and with the intent of simplifying the equations, the friction term is replaced by a linear damping term proportional to the velocity, $\mathbf{F} = \delta \mathbf{v}$, where $\delta$ is a damping coefficient to be specified. With this approximation the set of equations 7, 8 and 9 are complete and formally may be solved for

the velocity $\bar{v}_1$ and the surface pressure $p_{s1}$, assuming that the static pressure and temperature, $p_{s0}$ and $T_0$, and the motion inducing temperature field $T_1$ are known. From this point on the subscript 1 denoting the first order terms will be dropped.

Letting the first order temperature field be represented by a superposition of fields of the form

$$T = T_{\omega k}(\theta, \sigma)\, e^{i(\omega t + k\phi)} \tag{10}$$

solutions of equations 7 and 8 for $\bar{v}$ and $p_s$ of the same form will be sought. With $\mu = \cos\theta$ and the definitions,

$$G_{\omega k} = \frac{p_{s\,\omega k}}{p_{s0}} + \frac{\bar{T}_{\omega k}}{\bar{T}_0} \tag{11}$$

$$\bar{\Phi}^*_{\omega k} = \frac{\bar{T}_{\omega k}}{\bar{T}_0} \tag{12}$$

$$\zeta = \zeta_r + \zeta_i = \frac{\omega}{2\Omega} - i\,\frac{\delta}{2\Omega} \tag{13}$$

$$\omega' = \omega - i\,\delta \tag{14}$$

equations (7) and (8) can be reduced to

$$\frac{\partial}{\partial\mu}\left[\frac{1-\mu^2}{\zeta^2-\mu^2}\,\frac{\partial G_{\omega k}}{\partial\mu}\right] - \frac{i}{\zeta^2-\mu^2}\left[\frac{k^2}{1-\mu^2} + \frac{k}{\zeta}\,\frac{(\zeta^2+\mu^2)}{(\zeta^2-\mu^2)}\right] G_{\omega k} + \frac{4a^2\Omega^2}{R\bar{T}_0}\,\frac{\omega}{\omega'}\,G_{\omega k} = \frac{4a^2\Omega^2}{R\bar{T}_0}\,\frac{\omega}{\omega'}\,\bar{\Phi}^*_{\omega k} \tag{15}$$

where a is the radius of the planet.

Equation 15 is an inhomogeneous Laplace Tidal equation with a linear damping term. The homogeneous equation, without damping, has for its solutions the Hough functions which are the eigenfunctions associated with eigenvalues generally expressed in terms of "equivalent depths" (Chapman and Lindzen, 1970). This problem has been discussed extensively in the literature (see for example Longuet-Higgins, 1967). The temperature field $T_{\omega k}$ could be expanded in Hough function and the inhomogeneous equation solved in terms of the eigenfunctions. However, in this case the eigenvalues and eigenfunctions would be complex due to the damping term. Rather than expanding in Hough functions which are infinite series of Legendre functions, the temperature field and resultant pressure and wind fields will be expanded in terms of Legendre functions. For the problem under consideration, the Legendre function solution converges reasonably fast. The only difficulty is that in solving the momentum equation for the wind velocities there is an apparent singularity when damping is not included. A zero in the Hough function formulation cancels the pole, while in the Legendre function formulation each Legendre mode does not exactly cancel the pole but instead the sum of the modes is required. Since the solution in terms of Legendre functions converges rapidly and because of the damping term, the difficulty is a minor one.

For the wave number k the temperature component $T_{\omega k}$ is expanded in a series of Legendre functions $P_m^k(\mu)$,

$$T_{\omega k} = \sum_{m=k}^{\infty} \beta_{km}(\sigma)\, P_m^k(\mu) \tag{16}$$

where the vertical structure is contained in the coefficients $\beta_{km}(\sigma)$. Using equation (16) the geopotential function becomes

$$\bar{\Phi}^*_{\omega k} = \sum_{m=k}^{\infty} \bar{\beta}^*_{km} P^k_m(\mu) \tag{17}$$

where $\bar{\beta}^*_{km} = \bar{\beta}_{km} / \bar{T}_0$. If the surface pressure is assumed to be of the form

$$\frac{P_{s\omega k}}{P_0} = \sum_{m=k}^{\infty} \alpha^*_{km} P^k_m(\mu) \tag{18}$$

then from (11) and (12)

$$G_{\omega k} = \sum_{m=k}^{\infty} (\alpha^*_{km} + \bar{\beta}^*_{km}) P^k_m(\mu) = \sum_{m=k}^{\infty} C_{km} P^k_m(\mu). \tag{19}$$

Now substituting (17) and (19) into the tidal equation (15) the recursion relation for the complex amplitudes $\alpha^*_{km}$ is obtained;

$$\begin{aligned}
&\frac{m-k}{(2m-1)\left[m(m-1)-\frac{k}{\zeta}\right]}\left[\frac{m-k-1}{2m-3}\,\alpha^*_{km-2} + \frac{(m-1)^2(m+k)}{m^2(2m-1)}\,\alpha^*_{km}\right] \\
&\quad - \left[\zeta^2 \frac{m(m+1)-\frac{k}{\zeta}}{m^2(m+1)^2} - \frac{R\bar{T}_0}{4a^2\Omega^2}\,\frac{\omega'}{\omega}\right]\alpha^*_{km} \\
&\quad + \frac{m+k+1}{(2m+3)\left[(m+1)(m+2)-\frac{k}{\zeta}\right]}\left[\frac{(m+2)^2(m-k+1)}{(m+1)^2(2m-1)}\,\alpha^*_{km} + \frac{m+k+2}{2m+5}\,\alpha_{km+2}\right] = -\frac{R\bar{T}_0}{4a^2\Omega^2}\,\frac{\omega'}{\omega}\,\bar{\beta}^*_{km}.
\end{aligned} \tag{20}$$

Equation (20) represents an infinite set of equations for the coefficients $\alpha^*_{km}$. If the solution as represented by (18) converges then the set of equations can be

truncated to give a solution to the desired accuracy. The set of equations can be simplified somewhat by the introduction of auxiliary functions $\psi_{km}$ ,

$$\frac{(m+1)^2\,(m-k)}{m^2(2m-1)}\,\alpha_{km-1}+\frac{m+k+1}{2m+3}\,\alpha_{km+1}=\left(\frac{m+1}{m}-\frac{k}{\zeta m^2}\right)\psi_{km}. \tag{21}$$

Defining the following expressions;

$$K_{km}=\frac{(m+1)^2\,(m-k)}{(2m-1)\,m^2} \tag{22}$$

$$L_{km}=\frac{m+k+1}{2m+3} \tag{23}$$

$$N_{km}=\frac{m+1}{m}-\frac{1}{m^2}\,\frac{k}{\zeta} \tag{24}$$

$$M_{km}=\zeta^2\left[\frac{m+1}{m}-\frac{1}{m^2}\,\frac{k}{\zeta}\right]-(m+1)^2\,\frac{R\bar{T}_0}{4a^2\Omega^2} \tag{25}$$

and substituting into (20) and (21) the equations for the coefficients are,

$$K_{km}\psi_{km-1}-M_{km}\,\alpha^*_{km}+L_{km}\,\psi_{km+1}=-(m+1)^2\,\frac{R\bar{T}_0}{4a^2\Omega^2}\,\frac{\omega'}{\omega}\,\bar{\beta}^*_{km} \tag{26}$$

$$K_{km}\,\alpha^*_{km-1}-N_{km}\,\psi_{km}+L_{km}\,\alpha^*_{km+1}=0. \tag{27}$$

Equations (26) and (27) form two sets of equations, one set for odd and one set for even values of k-m. The even k-m modes are symmetric about the equator and odd k-m modes are asymmetric. In practice, (26) and (27) can be truncated and expressed in matrix form to solve for the finite set of $\alpha_{km}$ which

adequately represent the solution to the tidal equation. The approach used here closely parallels that used in the eigenfunction solution of the homogeneous tidal equation (Chapman and Lindzen, 1970).

Having solved for the $\alpha^*_{km}$ the pressure fluctuations are obtained from the assumed form in (10) and from (18).

$$p_s = p_0 \, e^{i(\omega t + k\phi)} \sum_{m=k}^{\infty} \alpha^*_{km} \, P^k_m(\mu) \tag{28}$$

with summation over the finite set of $\alpha^*_{km} P^k_m$ in practice. For multiple values of frequency $\omega$ and wave number k the solution is represented by a linear superposition of terms of the form in (28).

## POLAR SYMMETRIC FIELDS

The polar symmetric temperature field and the resultant pressure and wind fields can be regarded as zero wave number tidal theory. Because the time scale of any changes of these fields is much larger than the time scale of one day, the zero frequency limit of tidal theory can be used.

If k is made equal to zero in (20) where damping is implicit and the zero frequency limit is taken, the result is

$$\alpha^*_{0m} = -\overline{\beta}^*_{0m} \tag{29}$$

independent of the magnitude of the damping factor. On the other hand, taking the limit with $\delta$ equal to zero (no damping) the result is,

$$\frac{1}{(2m-1)(2m-3)}\,\alpha^*_{0m-2} + \left[\frac{R\bar{T}_0}{4a^2\Omega^2} - \frac{1}{(2m+3)(2m-1)} + \frac{1}{m(m+1)}\right]\alpha^*_{0m}$$

$$+ \frac{1}{(2m+3)(2m+5)}\,\alpha^*_{0m+2} = -\frac{R\bar{T}_0}{4a^2\Omega^2}\,\bar{\beta}^*_{0m}. \tag{30}$$

Thus, the limit of $\delta$ and $\omega$ approaching zero is not uniform. In the harmonic case with $\omega$ finite, the solutions are continuous functions of the damping parameter.

Considering the damped case as an initial value problem and applying the final value theorem, the result is identical to (29). The final value theorem does not apply to the undamped case. Assume that the initial velocity and pressure distributions are $\bar{\mathbf{v}}(0)$ and $p_{s1}(0)$ in (7) and (8). With the temperature applied as the step function $\{T_1 = 0,\ t < 0;\ T_1 = T(\theta, \sigma),\ t \geq 0\}$ and taking the Laplace transform of (7) and (8) using (9) and the linear damping term, the following set of equations is obtained,

$$s\tilde{\mathbf{v}}_1 - \mathbf{v}_1(0) + f\mathbf{k}\times\tilde{\mathbf{v}}_1 + \frac{R\bar{T}_0}{p_{s0}}\nabla\tilde{p}_{s1} + \delta\tilde{\mathbf{v}}_1 = -\frac{R}{s}\nabla\bar{T} \tag{31}$$

$$s\tilde{p}_{s1} - p_{s1}(0) + p_{s0}\nabla\cdot\tilde{\mathbf{v}}_1 = 0, \tag{32}$$

where s is the complex frequency and the tilde over a function represents its Laplace transform.

Equations (31) and (32) can be reduced to an equation analogous to the tidal equation (15);

$$\frac{\partial}{\partial\mu}\left(\frac{1-\mu^2}{\zeta^2-\mu^2}\,\frac{\partial\tilde{p}^*}{\partial\mu}\right)+\frac{s}{s+\delta}\,\frac{4a^2\Omega^2}{R\bar{T}_0}\,\tilde{p}^*=-\frac{1}{s}\,\frac{\partial}{\partial\mu}\left(\frac{1-\mu^2}{\zeta^2-\mu^2}\,\frac{\partial\bar{\Phi}^*}{\partial\mu}\right)$$

$$-\frac{s}{s+\delta}\,\frac{4a^2\Omega^2}{R\bar{T}_0}\left[\frac{1}{s}P_{s1}(0)+\frac{1}{s}\,\frac{s+\delta}{(s+\delta)^2+f^2}\,\nabla\cdot\left(\bar{\mathbf{v}}_1(0)-\frac{f}{s+\delta}\,\mathbf{k}\times\bar{\mathbf{v}}_1(0)\right)\right] \tag{33}$$

where $\tilde{p}^*$ is the Laplace transform of $p_{s1}/p_{s0}$, $\bar{\Phi}^* = \bar{T}/\bar{T}_0$, and $\zeta^2 = -(s+\delta)^2/4\Omega^2$. As was done previously $\bar{\Phi}^*$ and $\tilde{p}^*$ are expanded in Legendre functions, i.e.,

$$\bar{\Phi}^* = \sum_{m=1}^{\infty} \bar{\beta}_m^* P_m(\mu) \tag{34}$$

$$\tilde{p}^* = \sum_{m=1}^{\infty} \tilde{\alpha}_m^* P_m(\mu). \tag{35}$$

Substituting (34) and (35) into (33), the recursion relationship for the coefficients, $\tilde{\alpha}_m^*$, of the expansion of the Laplace transform of the pressure ratio is obtained;

$$\frac{1}{(2m-1)(2m-3)}\,\tilde{\alpha}_{m-2}^* - \left[\frac{s+\delta}{s}\,\frac{R\bar{T}_0}{4a^2\Omega^2} - \frac{1}{(2m+3)(2m-1)} - \frac{\zeta^2-1}{m(m+1)}\right]\tilde{\alpha}_m^*$$

$$+\frac{1}{(2m+3)(2m+s)}\,\tilde{\alpha}_{m+2}^* = -\frac{s+\delta}{s^2}\,\frac{R\bar{T}_0}{4a^2\Omega^2}\,\bar{\beta}^* + (\text{initial value terms}) \tag{36}$$

Assume for the moment that the initial values are zero. Let the coefficients $\tilde{\alpha}_m^*$ and $\bar{\beta}_m^*$ be written as column matrices of vectors in the form

$$\tilde{\boldsymbol{\alpha}} = \begin{pmatrix} \tilde{\alpha}_1^* \\ \tilde{\alpha}_2^* \\ \vdots \end{pmatrix} \tag{37}$$

$$\beta = \begin{pmatrix} \overline{\beta}_1^* \\ \overline{\beta}_2^* \\ \vdots \end{pmatrix}. \tag{38}$$

Then (36) can be written in matrix form as

$$A\tilde{\alpha} = -\frac{s+\delta}{s^2}\,\frac{R\overline{T}_0}{4a^2\Omega^2}\,\beta, \tag{39}$$

where A represents the matrix with diagonal and off-diagonal terms defined by

$$[A]_{m,m} = \frac{s+\delta}{s}\,\frac{R\overline{T}_0}{4a^2\Omega^2} - \frac{\zeta^2 - 1}{m(m+1)} - \frac{1}{(2m+3)(2m-1)} \tag{40}$$

$$[A]_{m,m+1} = \frac{1}{(2m+3)(2m+5)} \tag{41}$$

$$[A]_{m,m-1} = \frac{1}{(2m-1)(2m-3)}. \tag{42}$$

All other elements of A are zero. Using the final value theorem, (Gardner and Barnes, 1942) the time asymptotic solution for the inverse transform of the coefficients $\tilde{\alpha}_m^*$ is,

$$\alpha = \lim_{s\to 0} s\tilde{\alpha} = \lim_{s\to 0}\left(-\frac{s+\delta}{s}\,A^{-1}\beta\right). \tag{43}$$

It is assumed that the infinite matrix A can be truncated at a point which will adequately describe the transform $\tilde{\alpha}$ and the inverse transform $\alpha$.

Taking the limits $s \to 0$, the diagonal terms of A behave as $(\delta/s)\, R\bar{T}_0/4a^2\Omega^2$. The diagonal terms of $A^{-1}$ behave then as $(\delta/s)^{-1}\ 4a^2\,\Omega^2/R\bar{T}_0$ and the off-diagonal terms as $(\delta/s)^{-j}\ (4a^2\,\Omega^2/R\bar{T}_0)^j$ with $j > 1$. Using these limits

$$\lim_{s\to 0} \frac{s+\delta}{s}\ \frac{R\bar{T}_0}{4a^2\Omega^2}\ A^{-1} = I, \tag{44}$$

where I is the identity matrix. Therefore (43) reduces to the same results as expressed in (29).

If the initial values of $p_{s1}$ and $\bar{v}_1$ are not zero they will contribute terms to $\alpha$ of the form,

$$\lim_{s\to 0} A^{-1}\left[a_1 + \frac{s+\delta}{(s+\delta)^2 + f^2}\ a_2 + \frac{f}{(s+\delta)^2 + f^2}\ a_3\right] \tag{45}$$

where $a_1$, $a_2$ and $a_3$ depend on the initial values but are independent of s. In the limit these terms go to zero, and the final state is independent of the initial state.

To be physically realistic some dissipation should be present, and with the realization that the method by which the dissipation was introduced here may be oversimplified, the solutions to the polar symmetric equation will be assumed to be expressed by (29). Using this result along with the solutions to (26) and (27), the surface pressure can be obtained from the zero order quantities and the imposed first order temperature field.

VELOCITY FIELD

The calculated surface pressure and the imposed temperature field provide sufficient information to calculate the horizontal wind field as a function of latitude, local time and altitude. With $\nabla p_{s0}$ equal to zero and the friction term $\mathbf{F}$ replaced by the linear damping term $-\delta \mathbf{v}_1$, the momentum equation (4) becomes

$$\frac{\partial \mathbf{v}_1}{\partial t} + f\mathbf{k} \times \mathbf{v}_1 + \delta \mathbf{v}_1 = -\frac{RT_0}{p_{0s}} \nabla p_{s1} + \nabla \Phi_1 \tag{46}$$

For harmonic fields of the form $e^{i(\omega t + k\phi)}$, using (10) and (16) and the definition $\beta^*_{km} = \beta_{km}/RT_0$, (46) written in the form of the harmonic components $\mathbf{v}_{\omega k}$ of $\mathbf{v}_1$ is

$$i\omega \mathbf{v}_{\omega k} + f\mathbf{k} \times \mathbf{v}_{\omega k} + \delta \mathbf{v}_{\omega k} = \frac{RT_0}{a} \left[ \hat{\theta} \sqrt{1-\mu^2} \sum_{m=k} (\alpha^*_{km} + \beta^*_{km}) \frac{dP^k_m}{d\mu} \right.$$

$$\left. - \hat{\Phi} \frac{ik}{\sqrt{1-\mu^2}} \sum_{m=k} (\alpha^*_{km} + \beta^*_{km}) P^k_m \right] \tag{47}$$

$\hat{\theta}$ and $\hat{\Phi}$ are the unit vectors in the directions of increasing colatitude and east longitude. Taking $v_{\theta, \omega k}$ as the $\theta$ directed wind component, $v_{\phi, \omega k}$ as the $\phi$ directed component and using the definition (13), the expressions for the wind field from (47) are

$$v_{\phi,\omega k} = \frac{RT_0}{2\Omega a\left[(\mu^2 - \zeta_r^2 + \zeta_i^2)^2 + 4\zeta_r^2\zeta_i^2\right]} \frac{1}{\sqrt{1-\mu^2}} \sum_{m=k} (\alpha^*_{km} + \beta^*_{km}) \times$$

$$\left\{(\mu^2 - \zeta_r^2 + \zeta_i^2)\left[\zeta_r k P_m^k - \mu(1-\mu^2)\frac{dP_m^k}{d\mu}\right] - 2\zeta_r\zeta_i^2 k P_m^k\right.$$

$$\left. + 2i\zeta_r\zeta_i\left[\zeta_r k P_m^k - \mu(1-\mu^2)\frac{dP_m^k}{d\mu}\right] + i(\mu^2 - \zeta_r^2 + \zeta_i^2)k\zeta_i P_m^k\right\} \quad (48)$$

$$v_{\theta,\omega k} = \frac{RT_0}{2a\Omega\left[(\mu^2-\zeta_r^2+\zeta_i^2)^2+4\zeta_r^2\zeta_i^2\right]} \frac{1}{\sqrt{1-\mu^2}} \sum (\alpha^*_{km} + \beta^*_{km}) \times$$

$$\left\{-(\mu^2 - \zeta_r^2 + \zeta_i^2)(1-\mu^2)\zeta_i \frac{dP_m^k}{d\mu} - 2\zeta_r\zeta_i\left[-\mu k P_m^k + \zeta_r(1-\mu^2)\frac{dP_m^k}{d\mu}\right]\right.$$

$$\left. -2i\zeta_r\zeta_i^2(1-\mu^2)\frac{dP_m^k}{d\mu} + i(\mu^2 - \zeta_r^2 + \zeta_i^2)\left[-\mu k P_m^k + \zeta_r(1-\mu^2)\frac{dP_m^k}{d\mu}\right]\right\}. \quad (49)$$

Expressions (48) and (49) are superpositions of products of $\sigma$-dependent functions and $\mu$ (or latitudinal)-dependent functions. The $\mu$-dependent functions are defined as being zonal or meridional modes. The zonal modes are, using a prime to indicate the derivitive of the Legendre function

$$Z_{r,km} = \frac{1}{\sqrt{1-\mu^2}\left[(\mu^2 - \zeta_r^2 + \zeta_i^2)^2 + 4\zeta_r^2\zeta_i^2\right]}\left\{(\mu^2 - \zeta_r^2 + \zeta_i^2)\left[\zeta_r k P_m^k - \mu(1-\mu^2)P_m^{k\prime}\right]\right.$$

$$\left. -2\zeta_r\zeta_i^2 k P_m^k\right\} \quad (50)$$

$$Z_{i,km} = \frac{1}{\sqrt{1-\mu^2}\,[(\mu^2 - \zeta_r^2 + \zeta_i^2)^2 + 4\zeta_r^2\zeta_i^2]} \left\{(\mu^2 - \zeta_r^2 + \zeta_i^2)k\zeta_i P_m^k \right.$$

$$\left. + 2\zeta_r\zeta_i\,[\zeta_r k P_m^k - \mu(1-\mu^2)\,P_m^{k\prime}]\right\}. \qquad (51)$$

The meridional modes are,

$$M_{r,km} = \frac{1}{\sqrt{1-\mu^2}\,[(\mu^2 - \zeta_r^2 + \zeta_i^2)^2 + 4\zeta_r^2\zeta_i^2]} \left\{-(\mu^2 - \zeta_r^2 + \zeta_i^2)(1-\mu^2)\,\zeta_i P_m^{k\prime} \right.$$

$$\left. -2\zeta_r\zeta_i\,[-\mu k P_m^k + \zeta_r(1-\mu^2)\,P_m^{k\prime}]\right\} \qquad (52)$$

$$M_{i,km} = \frac{1}{\sqrt{1-\mu^2}\,[(\mu^2 - \zeta_r^2 + \zeta_i^2)^2 + 4\zeta_r^2\zeta_i^2]} \left\{-2\zeta_r\zeta_i^2(1-\mu^2)P_m^k + (\mu^2 - \zeta_r^2 + \zeta_i^2)\times \right.$$

$$\left. [-\mu k P_m^k + \zeta_r(1-\mu^2)\,P_m^{k\prime}]\right\}. \qquad (53)$$

The i subscripted zonal modes and the r subscripted meridional modes are due to the damping term and would be identically zero if there were no damping; the remaining modes would be simplified accordingly.

The $\sigma$-dependent functions or mode amplitudes are defined as

$$A_{r,km} = \frac{RT_0}{2a\Omega}\,[\mathrm{Re}(\alpha_{km}^*) + \beta_{km}] \qquad (54)$$

$$A_{i,km} = \frac{RT_0}{2a\Omega}\,\mathrm{Im}\,(\alpha_{km}^*). \qquad (55)$$

The real and imaginary parts of $\alpha^*_{km}$ are due to the complex coefficients in (26) and (27); the complex coefficients are again due to the damping and without damping $A_{i,km}$ is identically zero. Using the modes and mode amplitudes, (48) and (49) can be rewritten in condensed notation

$$v_{\phi,\omega k} = \sum_{m=k} [A_{r,km}Z_{r,km} - A_{i,km}Z_{i,km} + i(A_{r,km}Z_{i,km} + A_{i,km}Z_{r,km})] \tag{56}$$

$$v_{\theta,\omega k} = \sum_{m=k} [A_{r,km}M_{r,km} - A_{i,km}M_{i,km} + i(A_{r,km}M_{i,km} + A_{i,km}M_{r,km})] \tag{57}$$

In the polar symmetric case where $k = 0$ and $\zeta_r = 0$, the modes are:

$$Z_{0m} = -\frac{\mu\sqrt{1-\mu^2}}{\mu^2 + \zeta_i^2} P_m^{k\prime} \tag{58}$$

$$M_{0m} = -\frac{\sqrt{1-\mu^2}}{\mu^2 + \zeta_i^2} \zeta_i P_m^{k\prime}. \tag{59}$$

If there is no damping $\zeta_i = 0$, and the meridional mode is identically zero. The existence of the meridional polar symmetric wind depends upon the existence of damping, with the magnitude of the velocity depending on the damping parameter. The mode amplitude is from (29)

$$A_{0m} = \frac{RT_0}{2a\Omega}(\beta^*_{0m} - \bar{\beta}^*_{0m}), \tag{60}$$

and the polar symmetric winds can be written

$$v_{\theta,0m} = A_{0m} M_{0m} \tag{61}$$

$$v_{\phi,0m} = A_{0m} Z_{0m}. \tag{62}$$

The total wind field can be expressed using the expressions defined above,

$$v_\phi = \sum_\omega \sum_k \left[ \sum_{m=k} (A_{r,km} Z_{r,km} - A_{i,km} Z_{i,km}) \cos(\omega t + k\phi + \phi_{0,\omega k}) \right.$$
$$\left. - \sum_{m=k} (A_{r,km} Z_{i,km} + A_{i,km} Z_{r,km}) \sin(\omega t + k\phi + \phi_{0,\omega k}) \right] + \sum_{m=1} A_{0m} Z_{0m} \tag{63}$$

$$v_\theta = \sum_\omega \sum_k \left[ \sum_{m=k} (A_{r,km} M_{r,km} - A_{i,km} M_{i,km}) \cos(\omega t + k\phi + \phi_{0,\omega k}) \right.$$
$$\left. - \sum_{m=k} (A_{r,km} M_{i,km} + A_{i,km} M_{r,km}) \sin(\omega t + k\phi + \phi_{0,\omega k}) \right] + \sum_{m=1} A_{0m} M_{0m}. \tag{64}$$

The angle $\phi_{0,\omega k}$ is determined from local time of the temperature maximum for a particular set of values of $\omega$ and k. The $\omega$ and k summations are over the combinations of frequency and wavenumber used to describe the temperature field.

## HEATING AND VERTICAL VELOCITIES

The atmospheric heating consistent with the imposed temperature field can be calculated from the tidal winds and pressures obtained in the previous sections. The heat equation in $\sigma$-coordinates can be written

$$Q = c_p \frac{\partial T}{\partial t} + c_p \mathbf{v} \cdot \nabla T + c_p \dot{\sigma} \frac{\partial T}{\partial \sigma} - \frac{RT}{\sigma p_s} \left( p_s \dot{\sigma} + \sigma \frac{\partial p_s}{\partial t} + \sigma \mathbf{v} \cdot \nabla p_s \right) \tag{65}$$

and the vertical velocity $\dot{\sigma}$ is determined from

$$\dot{\sigma} = - \frac{1}{p_s} \int_1^\sigma \nabla \cdot (p_s \mathbf{v}) \, d\sigma - \frac{(\sigma - 1)}{p_s} \frac{\partial p_s}{\partial t} \tag{66}$$

Expanding in terms of the parameter $\epsilon$, the first order equations from (65) and (66) are

$$Q_1 = c_p \frac{\partial T_1}{\partial t} + \left( c_p \frac{\partial T_0}{\partial \sigma} - \frac{RT_0}{\sigma} \right) \dot{\sigma}_1 - \frac{RT_0}{p_{s0}} \frac{\partial p_{s1}}{\partial t} \tag{67}$$

$$\dot{\sigma}_1 = - \int_1^\sigma \nabla \cdot \mathbf{v}_1 \, d\sigma - \frac{(\sigma - 1)}{p_{s0}} \frac{\partial p_{s1}}{\partial t}. \tag{68}$$

From this point on the subscript 1 will be dropped, and the first order quantities will have no subscript.

In terms of the mode and amplitude functions defined in the previous section, the vertical velocity due to the polar symmetric fields are, from (62) and (68)

$$\dot{\sigma}_{0m} = \frac{\sqrt{1 - \mu^2}}{a} \frac{dM_{0m}}{d\mu} \int_1^\sigma A_{0m} \, d\sigma. \tag{69}$$

From (18), (56), (57), and (68) the vertical velocity associated with the diurnal motion is, to first order

$$\dot{\sigma}_{\omega k} = -\frac{1}{a}\sum_{\omega \neq k}\left\{-\sqrt{1-\mu^2}\left[\frac{dM_{r,km}}{d\mu}\int_1^\sigma A_{r,km}d\sigma - \frac{dM_{i,km}}{d\mu}\int_1^\sigma A_{i,km}d\sigma\right.\right.$$

$$\left. + i\frac{dM_{i,km}}{d\mu}\int_i^\sigma A_{r,km}d\sigma + i\frac{dM_{r,km}}{d\mu}\int_1^\sigma A_{i,km}d\sigma\right]$$

$$+\frac{ik}{\sqrt{1-\mu^2}}\left[Z_{r,km}\int_1^\sigma A_{r,km}d\sigma - Z_{i,km}\int_1^\sigma A_{i,km}d\sigma + iZ_{i,km}\int_1^\sigma A_{r,km}d\sigma\right.$$

$$\left.\left. + iZ_{r,km}\int_1^\sigma A_{i,km}d\sigma\right\} + \sum_{m\neq k} i\omega(\sigma-1)\,(\alpha^*_{r,km} + i\alpha^*_{i,km})\,P^k_m. \qquad (70)$$

Using the vertical velocity calculated from (69) and (70) the vertically averaged heating is calculated using (67). For the polar symmetric components the time derivitives are zero and the heating in terms of the mode functions is

$$\bar{Q}_{0m} = c_p\int_0^1\left(\frac{\partial T_0}{\partial\sigma} - \frac{R}{c_p}\frac{T_0}{\sigma}\right)\dot{\sigma}_{0m}d\sigma. \qquad (71)$$

The heating associated with a diurnal wave of wave number k and frequency $\omega$ is

$$\bar{Q}_{\omega k} = i\omega c_p\,\bar{T}_{\omega k} + c_p\int_0^1\left(\frac{\partial T_0}{\partial\sigma} - \frac{R}{c_p}\frac{T_0}{\sigma}\right)\dot{\sigma}_{\omega k}d\sigma - i\frac{R\bar{T}_0}{P_{s0}}\omega p_{s,\omega k} \qquad (72)$$

where $p_{s,\omega k}$ is obtained from (18).

In (72) both $\dot{\sigma}_{\omega k}$ and $p_{s,\omega k}$ are complex. $\bar{Q}_{\omega k}$ is then the sum of real, $\bar{Q}_{r,\omega k}$, and imaginary parts, $\bar{Q}_{i,\omega k}$, which when combined with the exponential frequency and wavenumber term gives the expression for the total heating,

$$\bar{Q} = \sum_{\omega} \sum_{k} [\bar{Q}_{r,\omega k} \cos(\omega t + k\phi + \phi_{0,\omega k}) - Q_{i,\omega k} \sin(\omega t + k\phi + \phi_{0,\omega k})] + \bar{Q}_{01} + \bar{Q}_{02}. \tag{73}$$

The above expression is the heating in ergs $gm^{-1}$ $sec^{-1}$ averaged over $\sigma$; multiplying this expression by the quotient of the surface pressure and the gravitational acceleration gives the heating in terms of ergs/$cm^2$ sec.

$$\bar{Q}_s = \frac{P_{s0}}{g} \bar{Q}. \tag{74}$$

Using the hydrostatic equation in $\sigma$-coordinates, $\partial z/\partial\sigma = -RT/g\sigma$, the vertical velocity in cm/sec is obtained as a function of $\dot{\sigma}$ and the rate of change of temperature;

$$\frac{dz}{dt} = -\frac{RT}{g\sigma} \dot{\sigma} - \frac{R}{g} \int_1^{\sigma} \left( \frac{1}{\sigma} \frac{dT}{dt} - \frac{T}{\sigma^2} \dot{\sigma} \right) d\sigma. \tag{75}$$

To first order in $\epsilon$,

$$\frac{dz}{dt} = -\frac{RT_0}{g\sigma} \dot{\sigma} - \frac{R}{g} \int_1^{\sigma} \left( \frac{1}{\sigma} \frac{\partial T}{\partial t} - \frac{T_0}{\sigma^2} \dot{\sigma} \right) d\sigma. \tag{76}$$

The required value of $\dot{\sigma}$ can be calculated from (69) and (70)

$$\dot{\sigma} = \dot{\sigma}_{01} + \dot{\sigma}_{02} + \sum_{\omega} \sum_{k} [\dot{\sigma}_{r,\omega k} \cos(\omega t + k\phi + \phi_{0,\omega k}) - \dot{\sigma}_{i,\omega k} \sin(\omega t + k\phi + \phi_{0,\omega k})] \tag{77}$$

and $\partial T/\partial t$ from (10) can be written

$$\frac{\partial T}{\partial t} = - \sum_{\omega} \sum_{k} \omega T_{\omega k} \sin (\omega t + k\phi + \phi_{0,\omega k}). \qquad (78)$$

## APPLICATIONS TO MEASURED TEMPERATURE FIELDS

The derivations of the previous sections will now be applied to the temperature measurements from the Mariner 9 infrared spectroscopy experiment. In the results to be presented here, the mean surface pressure was taken to be 5 mb, and the temperature distribution was assumed to be of the form

$$T(\sigma, \mu, \phi, t) = T_0(\sigma) + \beta_{01}(\sigma) P_1(\mu) + \beta_{02}(\sigma) P_2(\mu)$$

$$+ [\beta_{11}(\sigma) P_1^1(\mu) + \beta_{12}(\sigma) P_1^2(\mu)] \cos(\Omega t + \phi + \phi_0) \qquad (79)$$

The height dependent coefficients were chosen by fitting the model to the temperature field measured during dust storm conditions. The resulting temperature contours at approximately one scale height are shown in Figure 1 and can be compared with the measured temperature field given by Hanel, et al. (1972). Since the data cover only the local time interval between approximately 5:00 and 19:00 Martian local time, the model provides an interpolation for times outside this interval as well as for other data void regions in the northern hemisphere. Values of $\overline{\beta}^*_{km}$ and $\beta^*_{km}(\sigma)$ are given in Table 1; these parameters are related to the coefficients in (79) by $\beta^*_{km} = \beta_{km}/RT_0$, and $\overline{\beta}^*_{km}$ is the $\sigma$-averaged value of $\beta^*_{km}(\sigma)$.

The values of $\overline{\beta}^*_{km}$ are used in (26) and (27) to solve for the coefficients $\alpha^*_{km}$ of the Legendre function expansion of the pressure ratio defined by (18). The values of $\alpha_{11}$ through $\alpha_{16}$, with and without damping, are listed in Table 2; only the first six modes are used since they converge rapidly. Using these $\alpha^*_{km}$, the 5 mb average surface pressure and the harmonic form suggested by (10), the diurnal component of the pressure field is obtained (Figure 2). With damping the lowest pressure occurs between the equator and the latitude of the diurnal temperature maximum and lags the temperature maximum in local time.

Without damping the results would differ somewhat. The imaginary parts, which cause a phase shift in local time, and the real parts with even m, which are the equatorially asymmetric modes, are all identically zero. Therefore, the pressure low and vertically averaged temperature maximum would occur at the same local time and the pressure minimum would be approximately on the equator.

The polar symmetric pressure component is determined by $\beta^*_{0m}$ from (29). Adding the polar symmetric and the diurnal components, the surface pressure shown in Figure 4 is obtained.

The modes of the horizontal wind field are calculated using (50), (51), (52), (53), (58), and (59). Examples of low order axially symmetric modes are shown in Figure 4 and higher order diurnal modes in Figures 5 and 6. In all cases the dotted curve would be zero if there were no damping and there would be singularities in the solid curves at ±30° latitude in Figures 5 and 6.

The amplitude functions defined in (54), (55), and (60) are shown in Figures 7 and 8. From (54), (60) and table 2 the amplitude of modes 01, 02 and the real parts of modes 11 and 12 are linear functions of the difference in $\beta^*_{km}$ and all, or a large fraction of, its vertical average $\overline{\beta}^*_{km}$. This situation occurs because these modes are driven by the temperature field directly, manifested in the geopotential term, and indirectly through the surface pressure. All the other velocity modes are driven only by the surface pressure modes. Due to the behavior of these amplitude functions the components of the wind field associated with them change sign in the middle range of $\sigma$ values. Since these are the dominant modes, the horizontal wind pattern reverses direction in going from the surface to high altitudes.

From (63) and (64) the wind fields are calculated using the amplitude and mode functions. The near surface winds are shown in Figure 9, the one scale height winds in Figure 10 and the high altitude winds in Figure 11. In comparing Figures 9 and 11 the wind reversal is obvious. Near the surface the average zonal flow is to the west in the northern winter hemisphere and to the east, but diminished, in the southern summer hemisphere. The average surface meridional flow is from north to south in both hemispheres but stronger in the northern hemisphere. At higher altitudes these averaged flows are reversed.

Vertical velocities are calculated using (76) with the results shown in Figure 12. The vertical velocity contours are similar but shifted 90° from the surface pressure contours. The dependence on the surface pressure is apparent

from the last term of equation (66). The dependence on the divergence of the velocity is more complicated and somewhat weaker. The effect of the polar symmetric fields is smaller than the diurnal components and is not readily apparent except near the poles. The polar symmetric vertical flow is downward from the north pole to within 10° north of the equator then upward to approximately 75° south and then downward again to the south pole. This behavior is due to a combination of two symmetric pole to equator meridional cells and a pole to pole cell.

The total atmospheric heating per vertically averaged column as calculated from (73) and (74) is shown in Fig. 13. This represents the total heating necessary to maintain the observed temperature field and calculated velocity field. It is of interest to examine separately, the dynamic contributions to the heating. The contribution due to vertical motion which is the second term in the right hand side of (67) is given in Figure 14, while Figure 15 shows the contribution due to the time rate of change of pressure or third term on the right hand side of (67). The dynamic contributions are both small compared to the total heating. In order to account for the required atmospheric heating at sub-solar latitudes (20°S) and local noon, the energy deposited in the atmosphere would amount to approximately 20% of the solar flux incident normally on the top of an atmospheric column. In order to achieve adequate night time cooling, an effective atmospheric emissivity of 0.53 would be required, assuming radiation to space (with an effective temperature of 200K) is the principle energy loss mechanism.

SUMMARY

The major dynamic effect produced by the observed diurnal temperature variation is the generation of diurnal pressure fluctuations (12% peak-to-peak) which are large by terrestrial standards. The resulting diurnal winds near the surface have amplitudes no greater than about 20 m/sec. Therefore, these winds alone are not capable of raising dust (Hess, 1972; Sagan and Pollack, 1967) and could not sustain the dust storm alone. However, by augmenting the polar symmetric wind fields or orographic wind fields, the diurnal winds could contribute to the raising of appreciable amounts of dust.

The 70-100 m/sec zonally symmetric winds in the latitude belt between 30° north and 30° south, which are the result of the latitudinal temperature gradient, could contribute to the lifting of dust into the atmosphere. However, these winds are strongly dependent on the magnitude of the damping parameter employed in the model. Although the surface streak patterns observed in the Mariner 9 television pictures (Sagan, et al., 1973) give support to the existance of the predicted wind pattern, the actual speed is indeterminate.

The mechanism producing the diurnal temperature fluctuations is not yet fully understood. Tidal resonance amplification does not appear to be a significant factor; except for the winter polar region, dynamic heating is a small part of the total atmospheric heating required. While the heating appears to be primarily a radiative effect, the large infrared atmospheric emissivity required to produce adequate cooling at night does not seem to be entirely consistent with the observed infrared spectra (Hanel, et al., 1972).

The linearized dynamic model employed in this study assumes a smooth spherical planet and treats frictional forces only through the use of linear damping. However, such a model should be adequate for estimating the gross properties of the wind fields from the observed temperature fields, and the results should provide guidance in the construction of more sophisticated models. Future models should include a more realistic treatment of the effects of frictional forces on the polar symmetric wind field. Because of the substantial large scale topographic relief on Mars, orographic effects may play a significant role in atmospheric dynamics (Blumsack, 1971; Gierasch and Sagan, 1971; Sagan, et al. 1971; Blumsack, et al., 1973), and these effects should also be included in future dynamical studies.

ACKNOWLEDGEMENT

The authors are grateful to Drs. R. A. Hanel, V. Kunde, and J. Pearl for their extensive contributions to the analysis and interpretation of the IRIS data and to Drs. C. Leovy and P. Gierasch for helpful discussions.

## REFERENCES


Blumsack, S. L., 1971: On the effects of topography on planetary atmospheric circulation. J. Atmos. Sci., 28, 312-318.

Blumsack, S. L., P. J. Gierasch and W. R. Wessel, 1973: An analytical and numerical study of the Martian planetary boundary layer over slopes. J. Atmos. Sci., 30, 66-82.

Chapman, S., and R. S. Lindzen, 1970: Atmospheric tides. Dordrecht, Holland, Reidel Publ. Co., 200 pp.

Gardner, M. F., and J. L. Barnes, 1942: Transients in Linear Systems. J. Wiley & Sons, Inc., New York, 389 pp.

Gierasch, P., and C. Sagan, 1970: A preliminary assessment of Martian wind regimes. Icarus, 14, 312-318.

Hanel, R., et al., 1972: Investigation of the Martian environment by infrared spectroscopy on Marine 9. Icarus, 17, 423-442.

Hess, S. L., 1972: Martian wind and dust clouds. NATO Advanced Study Institute on Planetary Atmospheres, Istanbul, Turkey.

Longuet-Higgins, M. S., 1967: The eigenfunctions of Laplace's tidal equations over a sphere. Phil. Trans. Roy. Soc., A262, 511-607.

Phillips, N. A., 1957: A coordinate system having some special advantages for numerical forecasting. J. Meteor., 14, 184-185.

Sagan, C., and J. B. Pollack, 1967: A windblown dust model of Martian surface features and seasonal changes. Smithsonian Astrophys. Obs. Special Report 255, 44 pp.

Sagan, C., J. Veverka, P. Gierasch, 1971: Observational consequences of Martian wind regime. Icarus, 15, 253-258.

Sagan, C., P. Fox, R. French, R. Dubisch, P. Gierasch, L. Quam, J. Lederberg, E. Levinthal, R. Tucker, D. Eross, J. Pollack, 1973. Variable features on Mars: Mariner 9 global results. Paper presented at AAS Division of Planetary Sciences Annual Meeting, 20-23 March, Tucxon, Arizona.

Table 1. Coefficients of the Legendre functions in the normalized geopotential function. Normalization is with respect to $RT_0$. The $\sigma$-averaged coefficients are normalized to $R\overline{T}_0$.

| $\sigma$ | $\beta^*_{01}$ | $\beta^*_{02}$ | $\beta^*_{01}$ | $\beta^*_{12}$ |
|---|---|---|---|---|
| 1.0 | 0.0 | 0.0 | 0.0 | 0.0 |
| 0.9 | -0.0206 | -0.0069 | 0.0054 | -0.0024 |
| 0.8 | -0.0434 | -0.0146 | 0.0120 | -0.0052 |
| 0.7 | -0.0689 | -0.0233 | 0.0199 | -0.0083 |
| 0.6 | -0.0979 | -0.0333 | 0.0297 | -0.0120 |
| 0.5 | -0.1314 | -0.0449 | 0.0420 | -0.0163 |
| 0.4 | -0.1714 | -0.0589 | 0.0577 | -0.0215 |
| 0.3 | -0.2212 | -0.0766 | 0.0788 | -0.0282 |
| 0.2 | -0.2879 | -0.1005 | 0.1093 | -0.0374 |
| 0.1 | -0.3925 | -0.1384 | 0.1607 | -0.0522 |
| | $\overline{\beta}^*_{01}$ | $\overline{\beta}^*_{02}$ | $\overline{\beta}^*_{11}$ | $\overline{\beta}^*_{12}$ |
| | -0.1709 | -0.0595 | 0.0638 | -0.0221 |

Table 2. Real and imaginary parts of the coefficients in the Legendre function expansion of the normalized pressure ratio. The relationship between the diurnal pressure modes (1, 1) to (1, 6) and the averaged geopotential modes (1, 1) and (1, 2) are shown with and without damping.

| | With Damping | Without Damping |
|---|---|---|
| Re | $\alpha^*_{11} = -0.6141\ \overline{\beta}^*_{11}$ | $-0.6254\ \overline{\beta}^*_{11}$ |
| Re | $\alpha^*_{12} = -0.6387\ \overline{\beta}^*_{12}$ | 0 |
| Re | $\alpha^*_{13} = 0.1054\ \overline{\beta}^*_{11}$ | $0.1095\ \overline{\beta}^*_{11}$ |
| Re | $\alpha^*_{14} = 0.0681\ \overline{\beta}^*_{12}$ | 0 |
| Re | $\alpha^*_{15} = -0.0061\ \overline{\beta}^*_{11}$ | $-0.0067\ \overline{\beta}^*_{11}$ |
| Re | $\alpha^*_{16} = -0.0030\ \overline{\beta}^*_{12}$ | 0 |
| Im | $\alpha^*_{11} = 0.1482\ \overline{\beta}^*_{11}$ | 0 |
| Im | $\alpha^*_{12} = 0.4520\ \overline{\beta}^*_{12}$ | 0 |
| Im | $\alpha^*_{13} = 0.0025\ \overline{\beta}^*_{11}$ | 0 |
| Im | $\alpha^*_{14} = -0.0272\ \overline{\beta}^*_{12}$ | 0 |
| Im | $\alpha^*_{15} = -0.0016\ \overline{\beta}^*_{11}$ | 0 |
| Im | $\alpha^*_{16} = 0.0004\ \overline{\beta}^*_{12}$ | 0 |

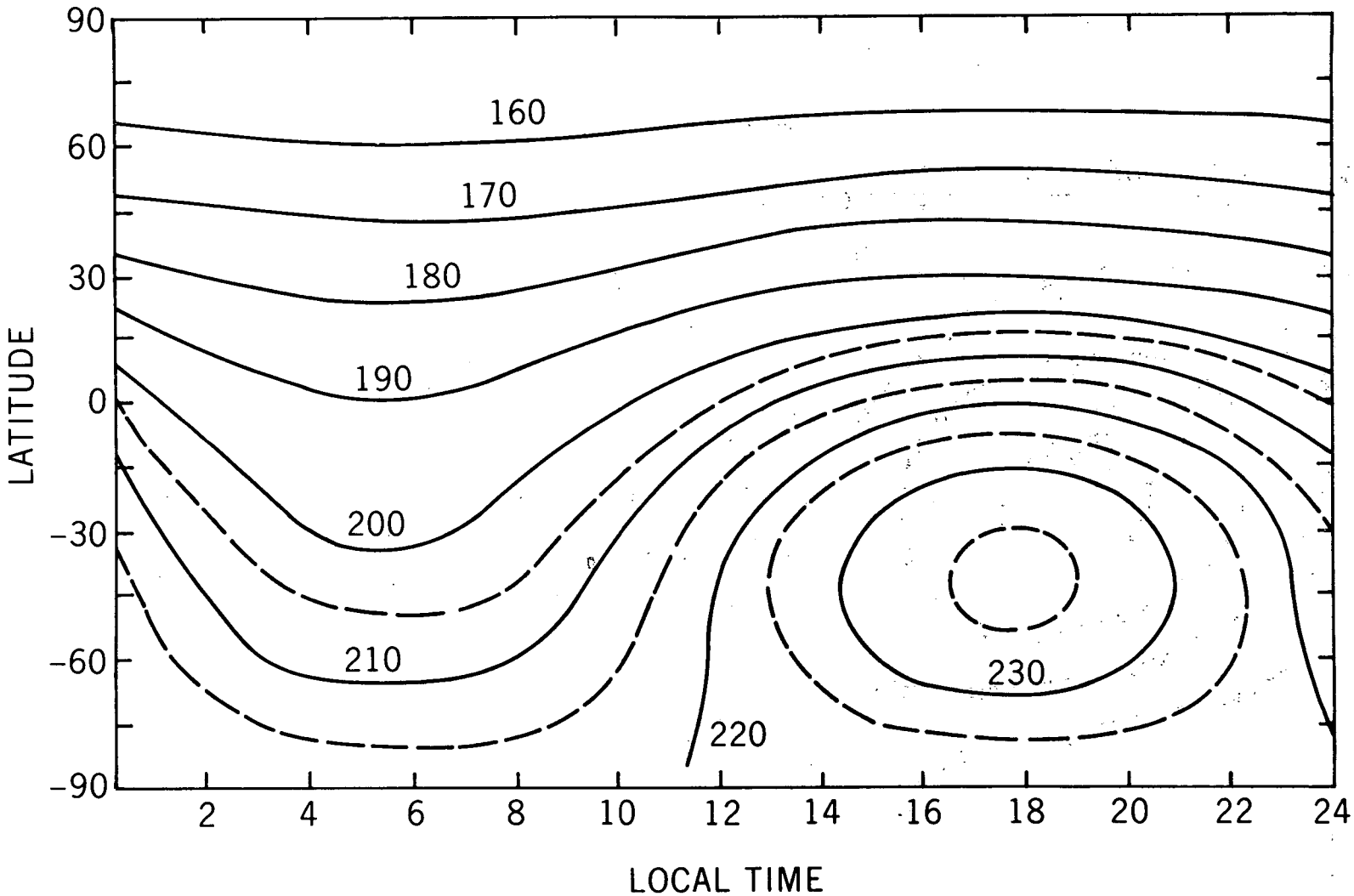


Figure 1. Model temperature field contours at one scale height. The temperature is expressed in degrees Kelvin.

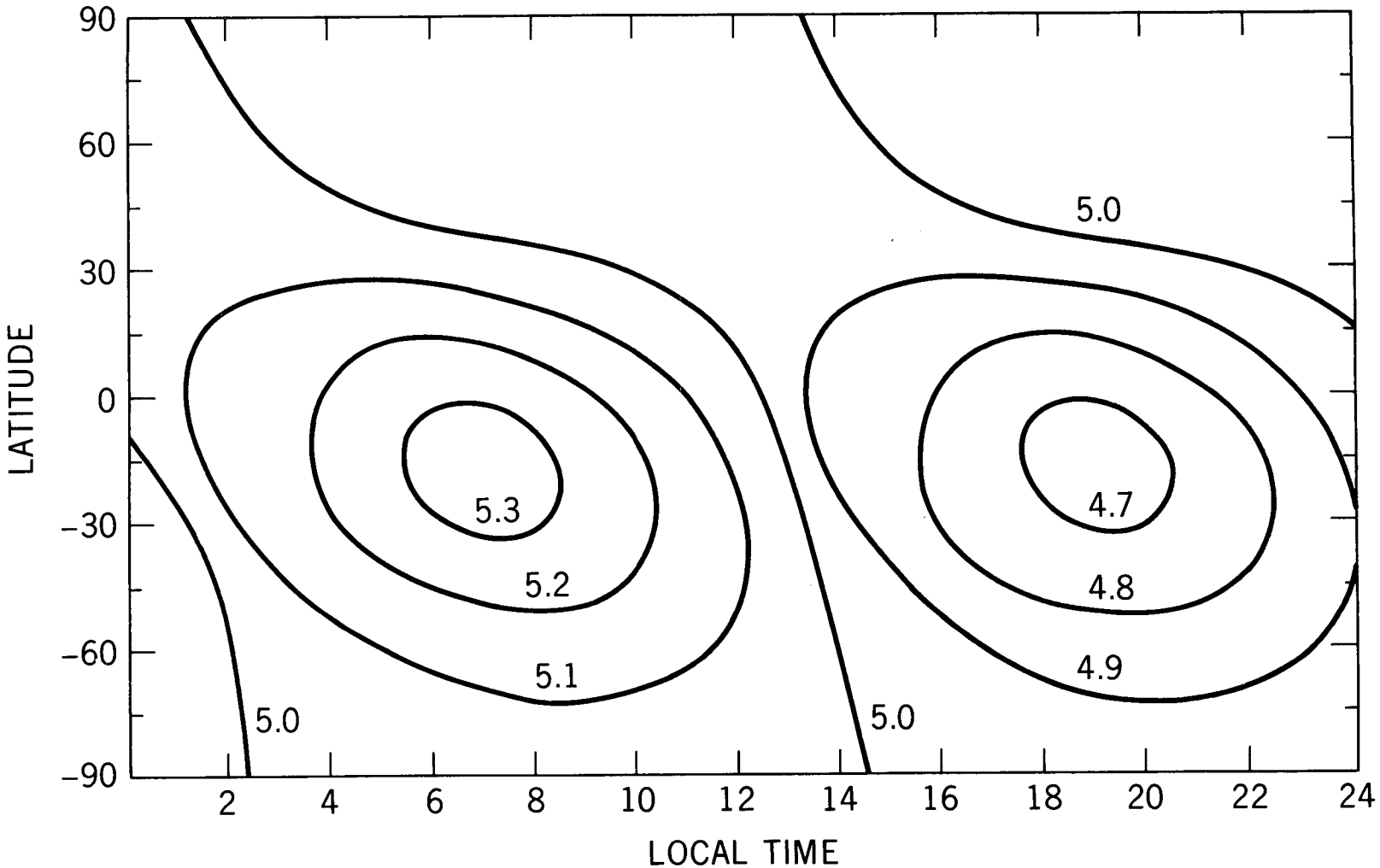


Figure 2. Contours of the diurnal component of the tidal surface pressure expressed in millibars. The average surface pressure is assumed to be 5 mb.

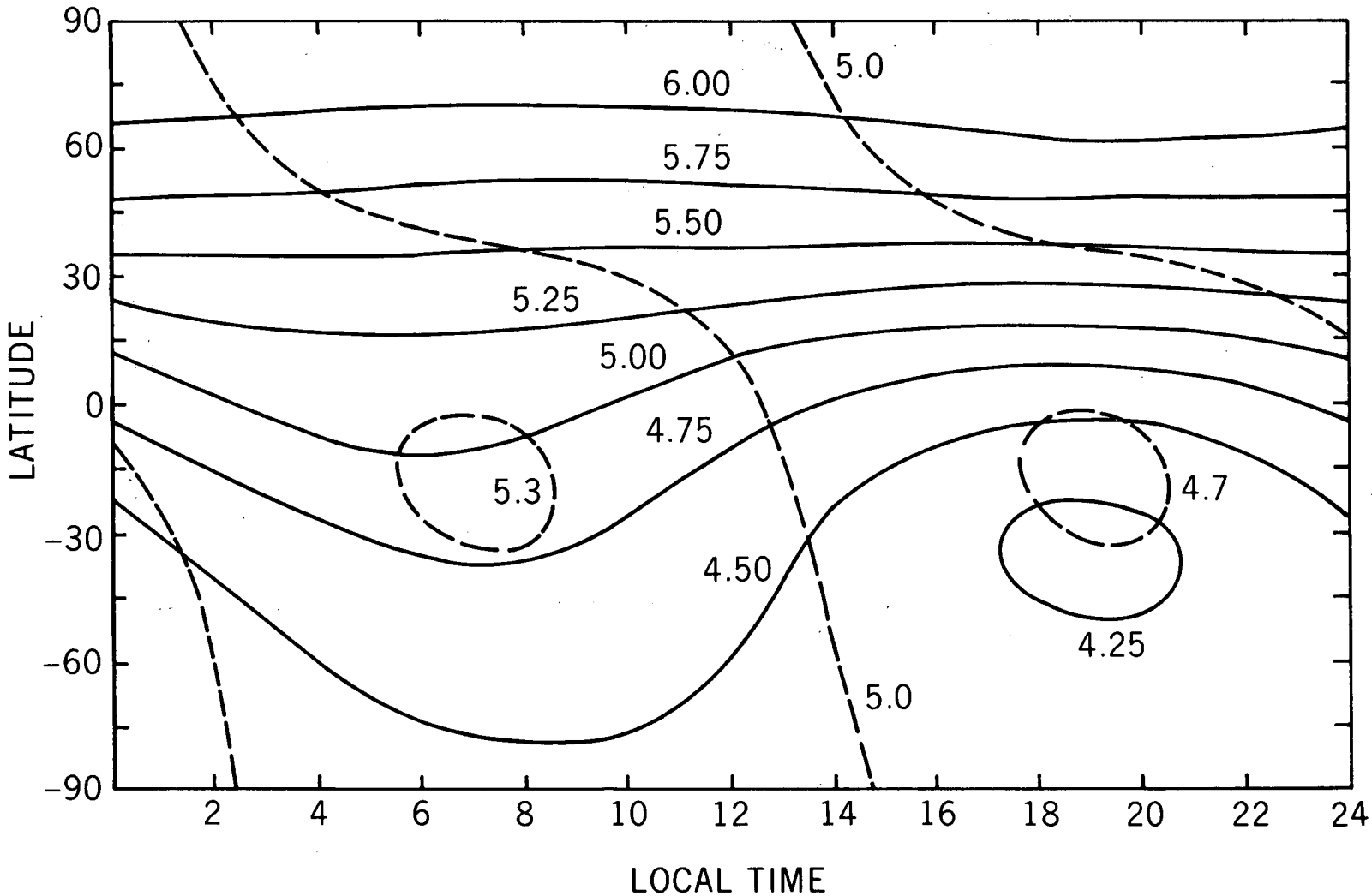


Figure 3. Contours of the total surface pressure. The pressure is the sum of the diurnal and zonally symmetric modes. The pressure is expressed in millibars and the average surface pressure is assumed to be 5 mb.

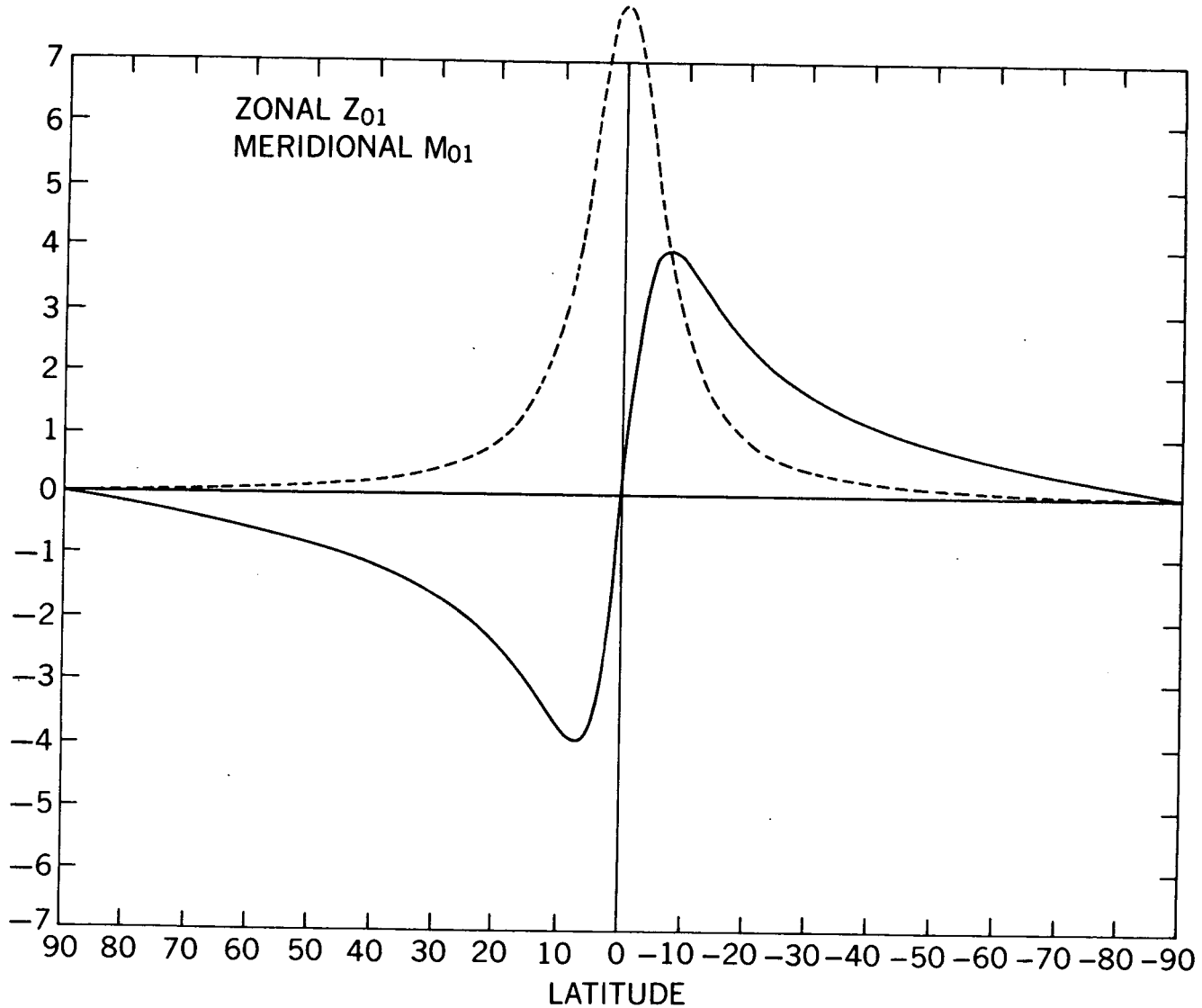


Figure 4. Zonally symmetric mode of the wind field. The product of the ordinate and the mode amplitude shown in Figure 7 gives the wind speed. $Z_{01}$ represents the zonal wind and $M_{01}$ the meridional wind which is the result of damping in the momentum equation.

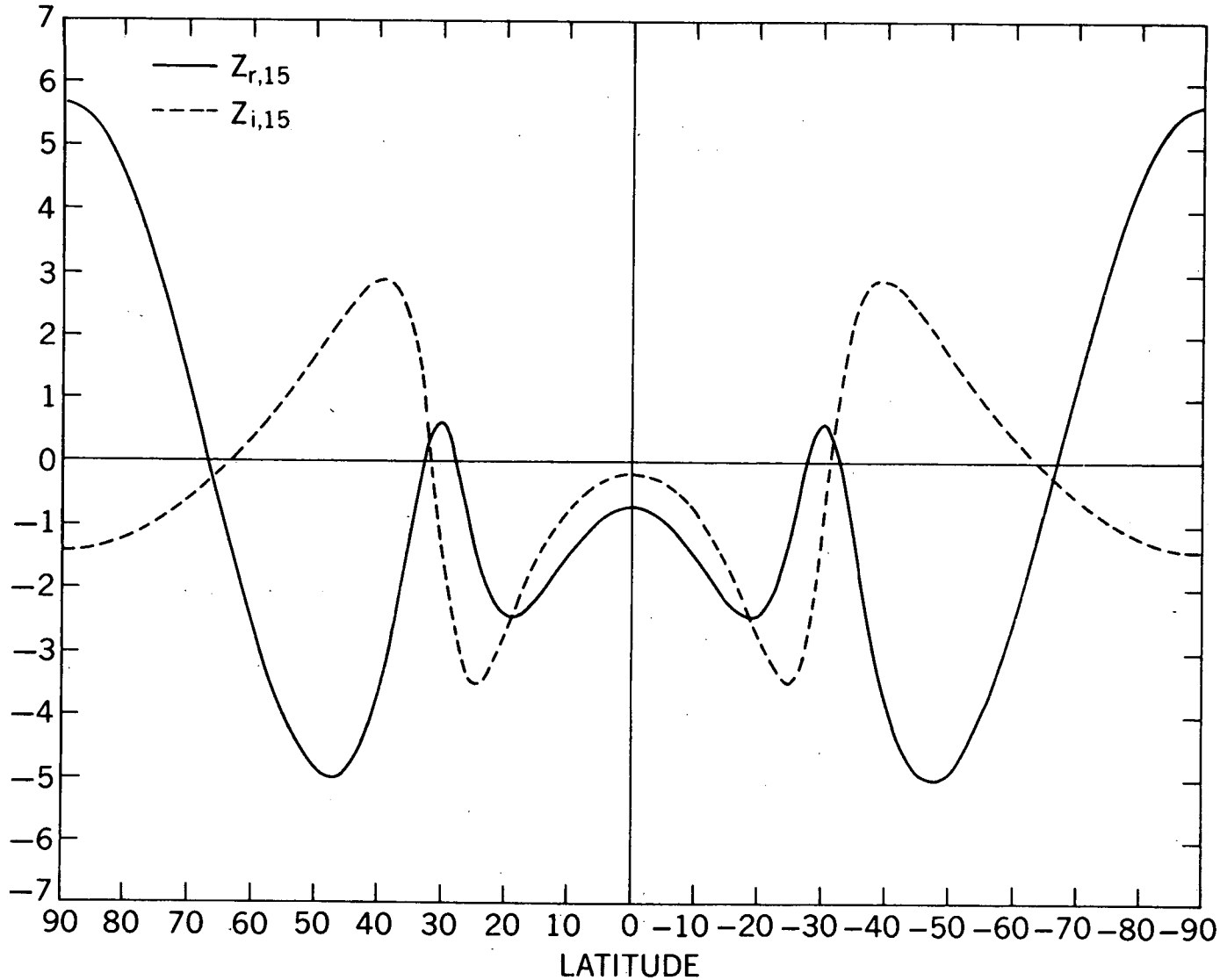


Figure 5. Symmetric mode (1, 5) of the zonal wind. The solid line is the temperature phased component. The dashed line is the out of phase component due to damping. The product of the ordinate and the mode amplitude shown in Figure 8 gives the mode wind speed.

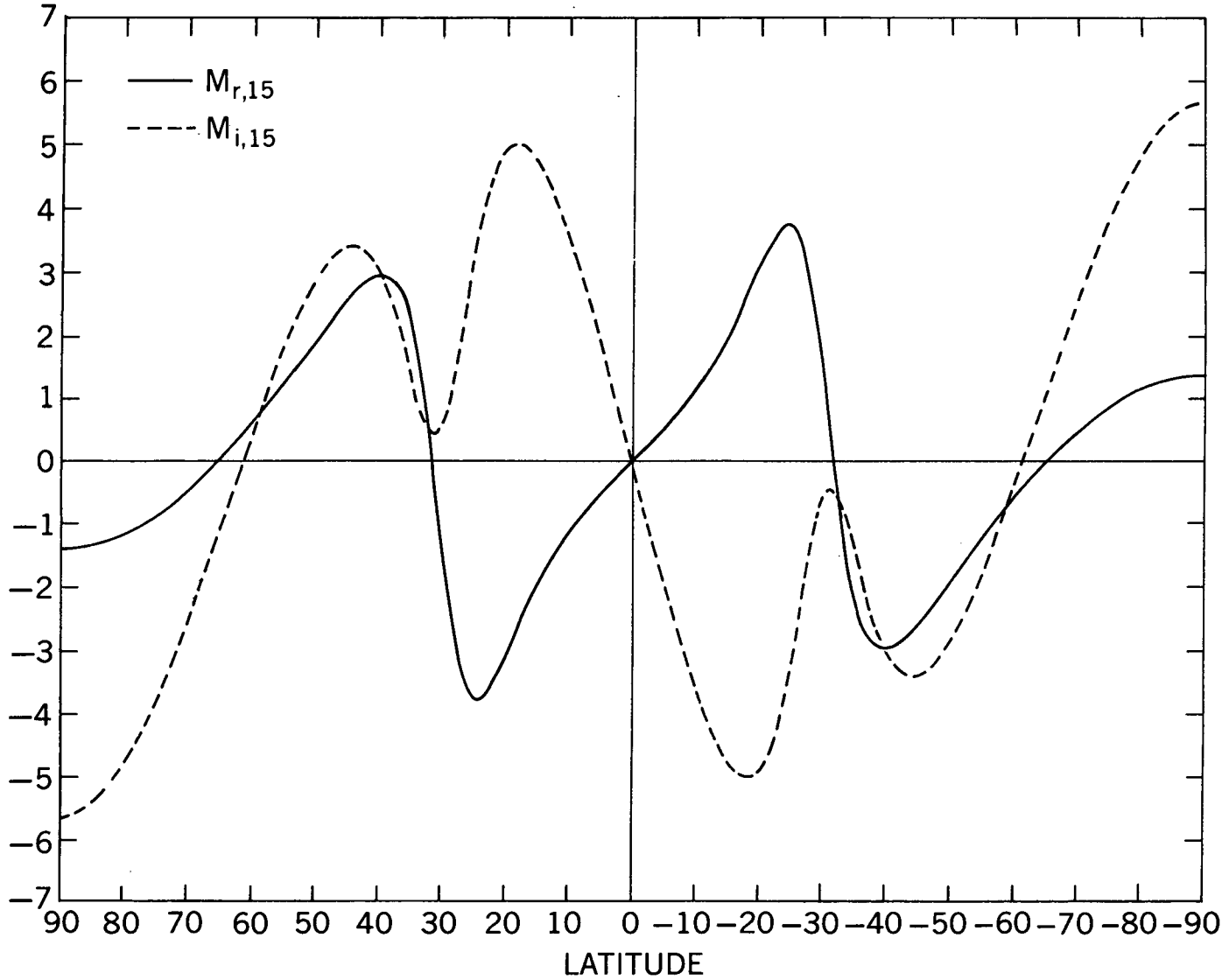


Figure 6. Similar to Figure 5 but for the meridional wind.

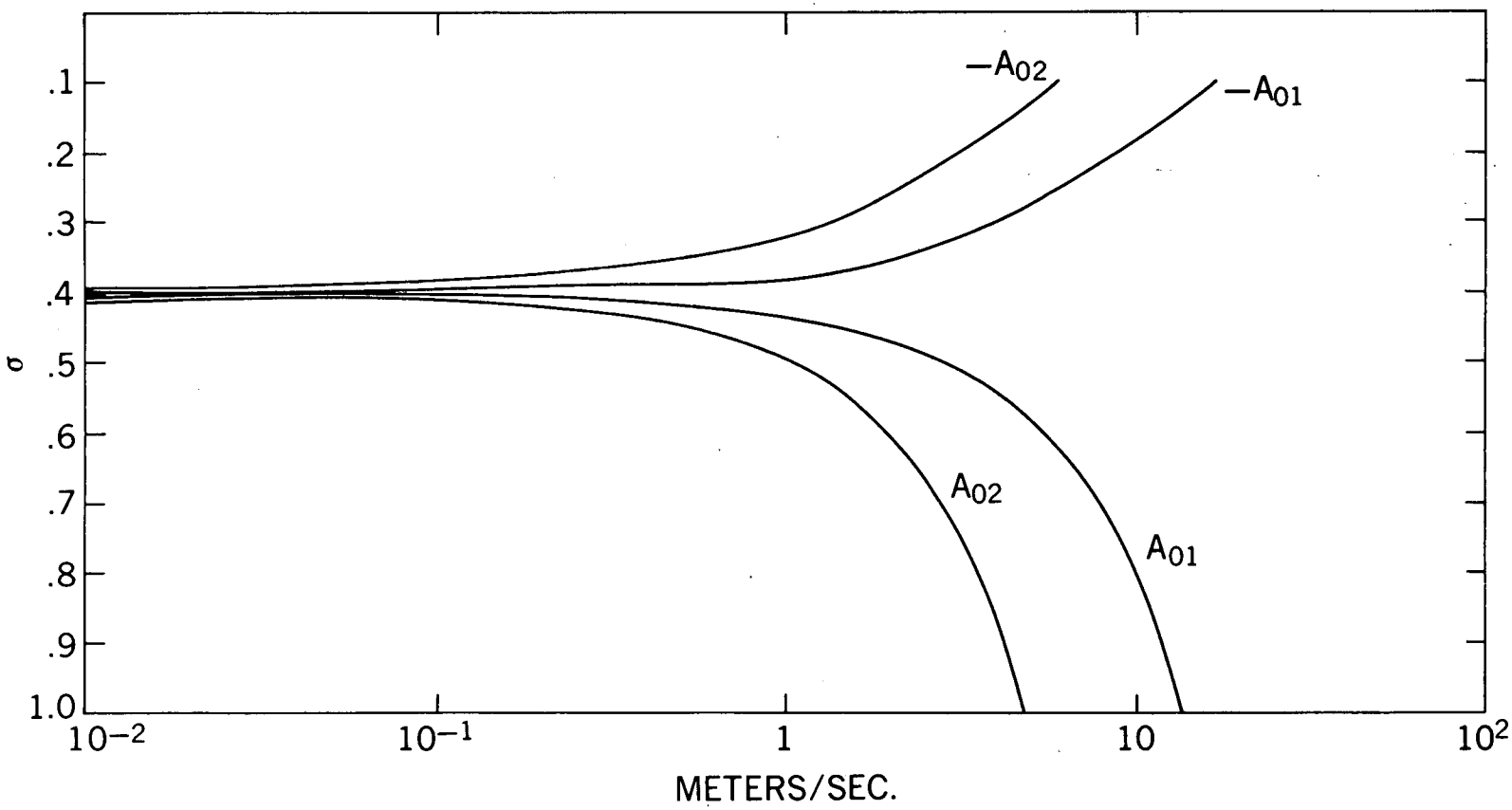


Figure 7. Amplitudes of the zonally symmetric modes. At approximately $\sigma = .4$ the amplitudes change sign indicating the reversal of the wind directions.

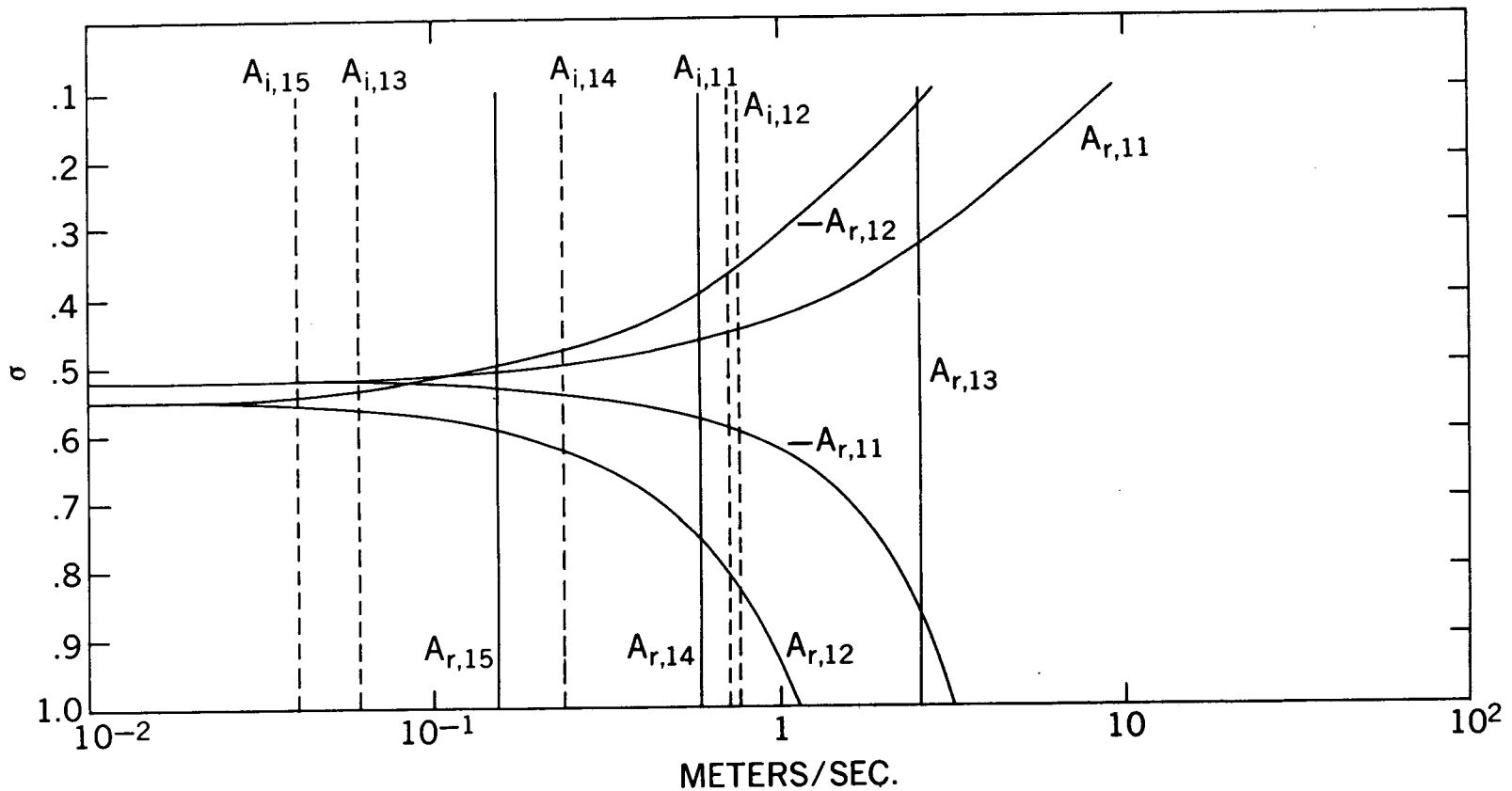


Figure 8. Amplitudes of the diurnal wind field modes. The sign of the real parts of $A_{11}$ and $A_{12}$ change between $\sigma = .5$ and .6 indicating the reversal of the modal wind field. The imaginary parts of all the mode amplitudes, shown dashed, are identically zero if no damping is assumed.

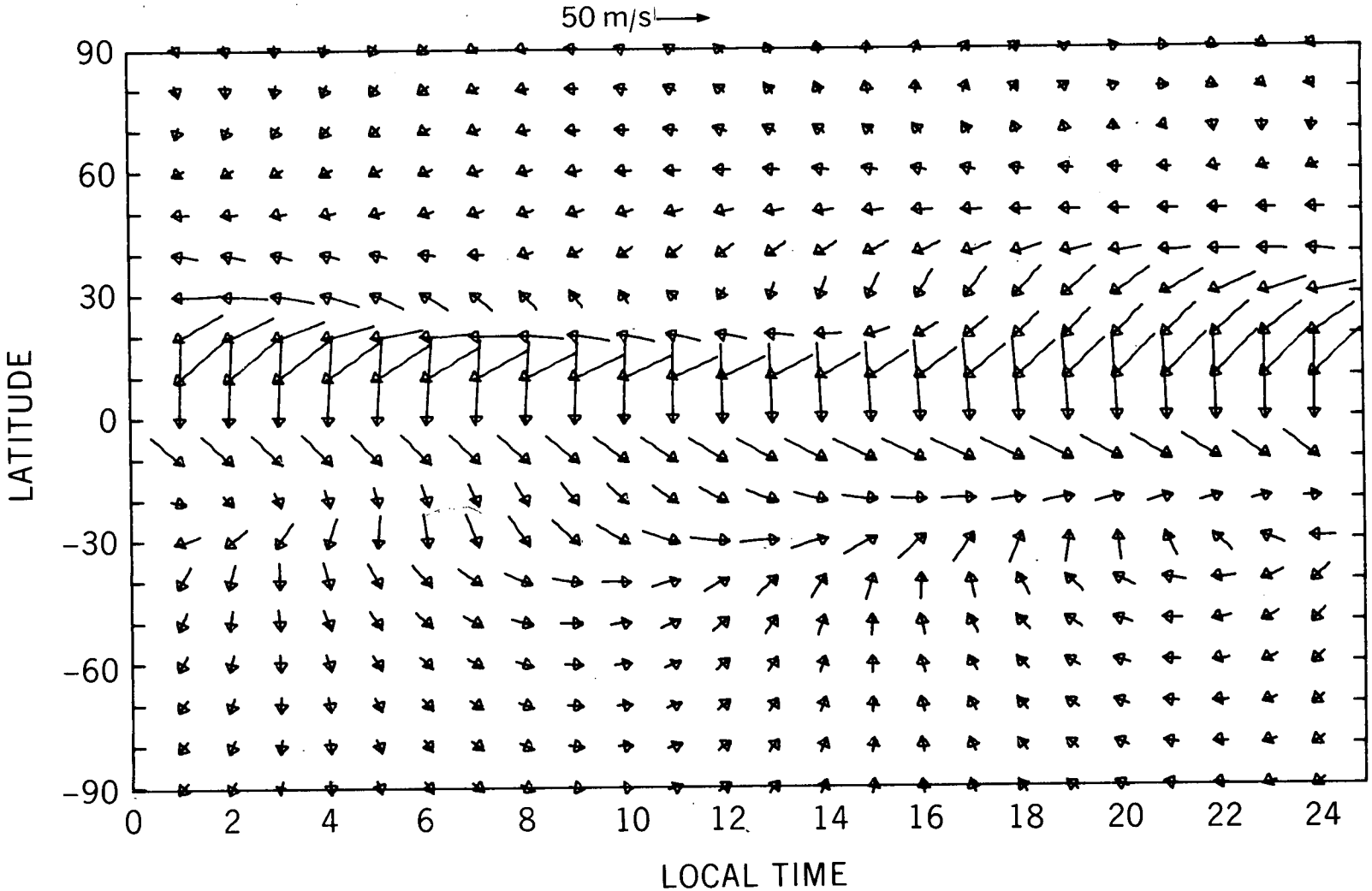


Figure 9. Near surface winds during the dust storm. The wind field is generated by the model temperature field based on the measured temperatures and the associated surface pressure. Wind amplitudes are scaled to the labeled vector.

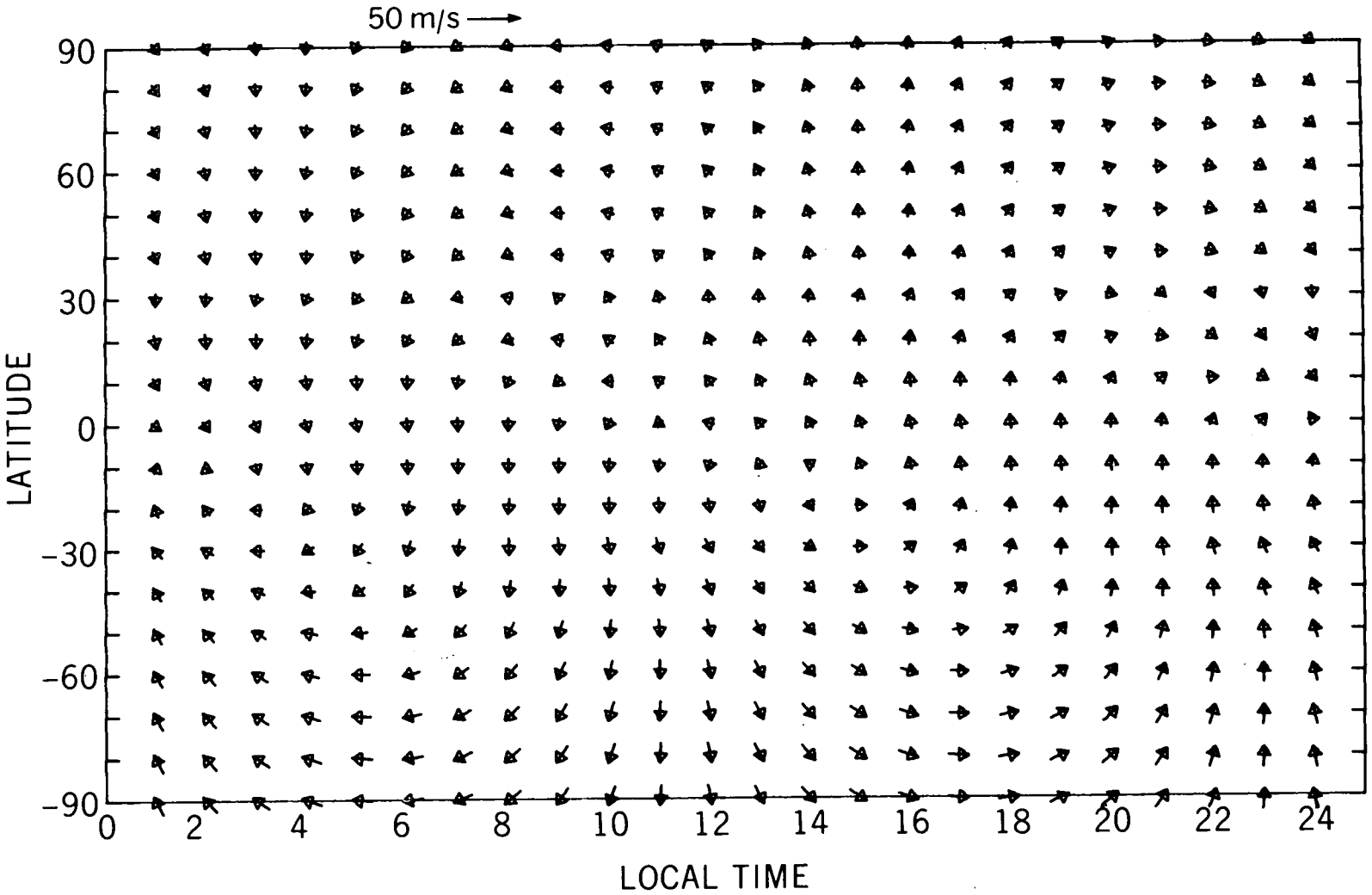


Figure 10. One scale height winds under same conditions as in Figure 9.

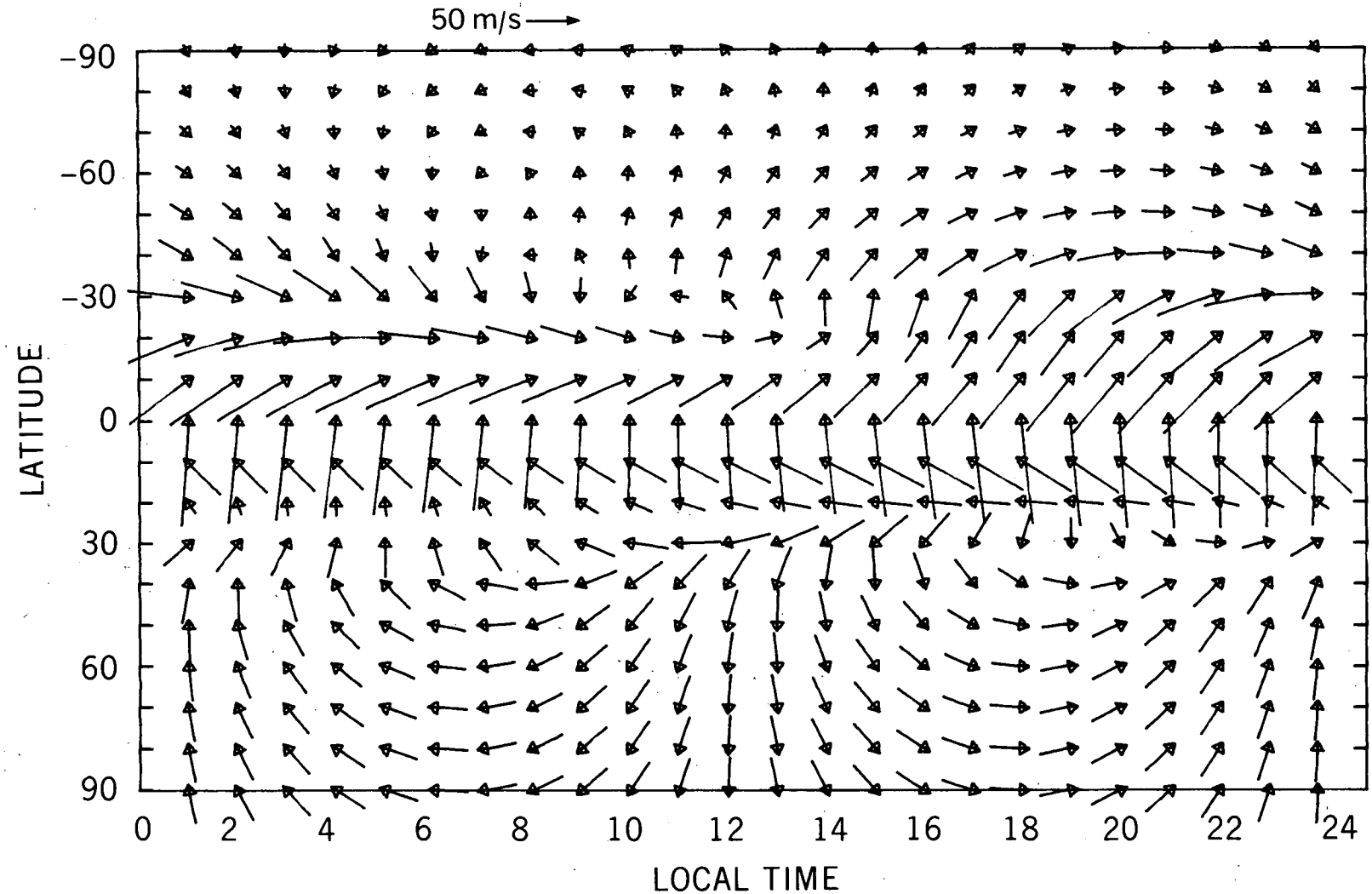


Figure 11. High altitude winds under same conditions as in Figure 9. The wind directions are generally reversed from those near the surface.

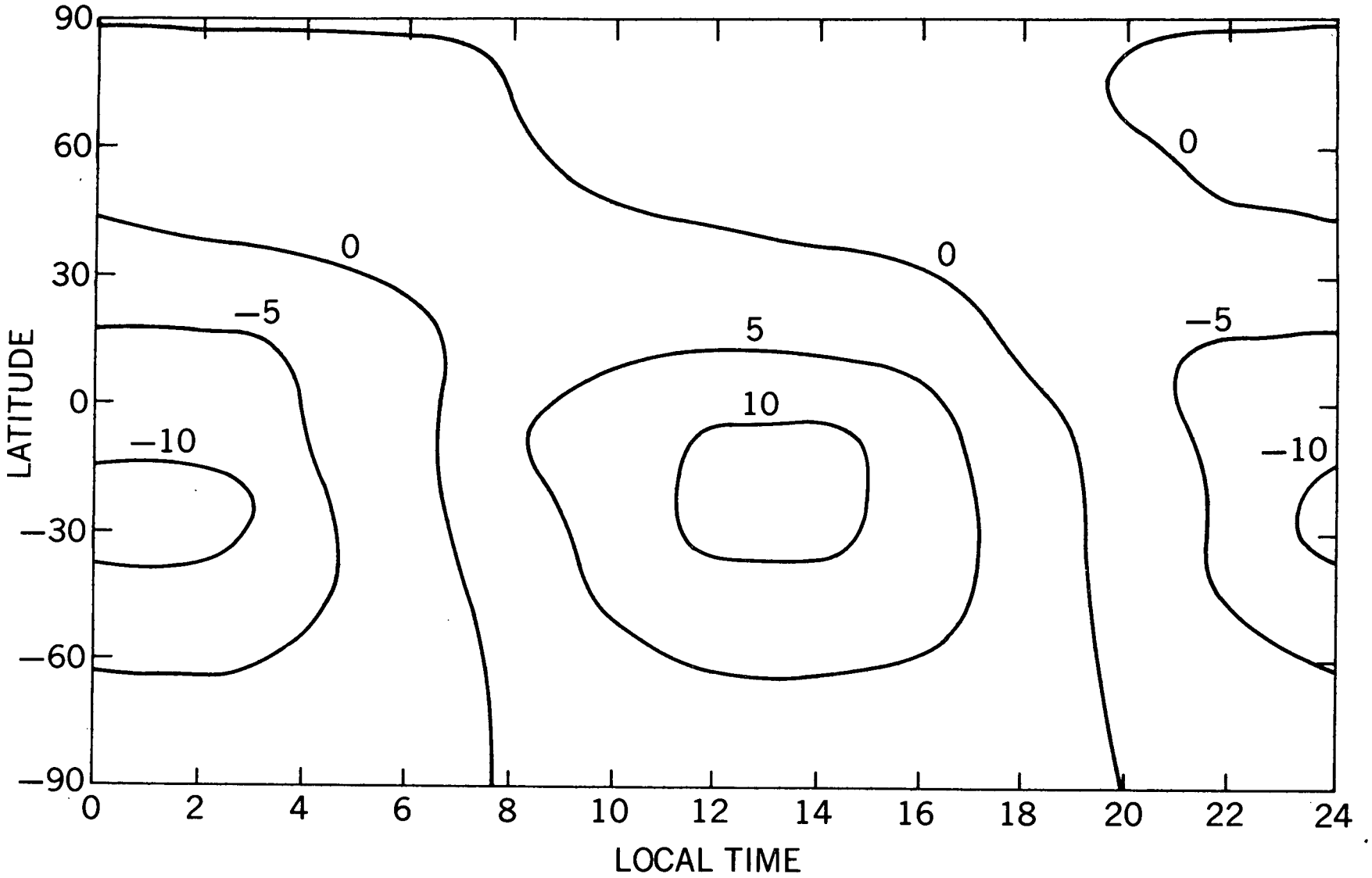


Figure 12. Vertical velocities of one scale height. The contours are similar to those of the diurnal surface pressure, shown in Figure 2, shifted by six hours in local time. The velocity is in cm/sec.

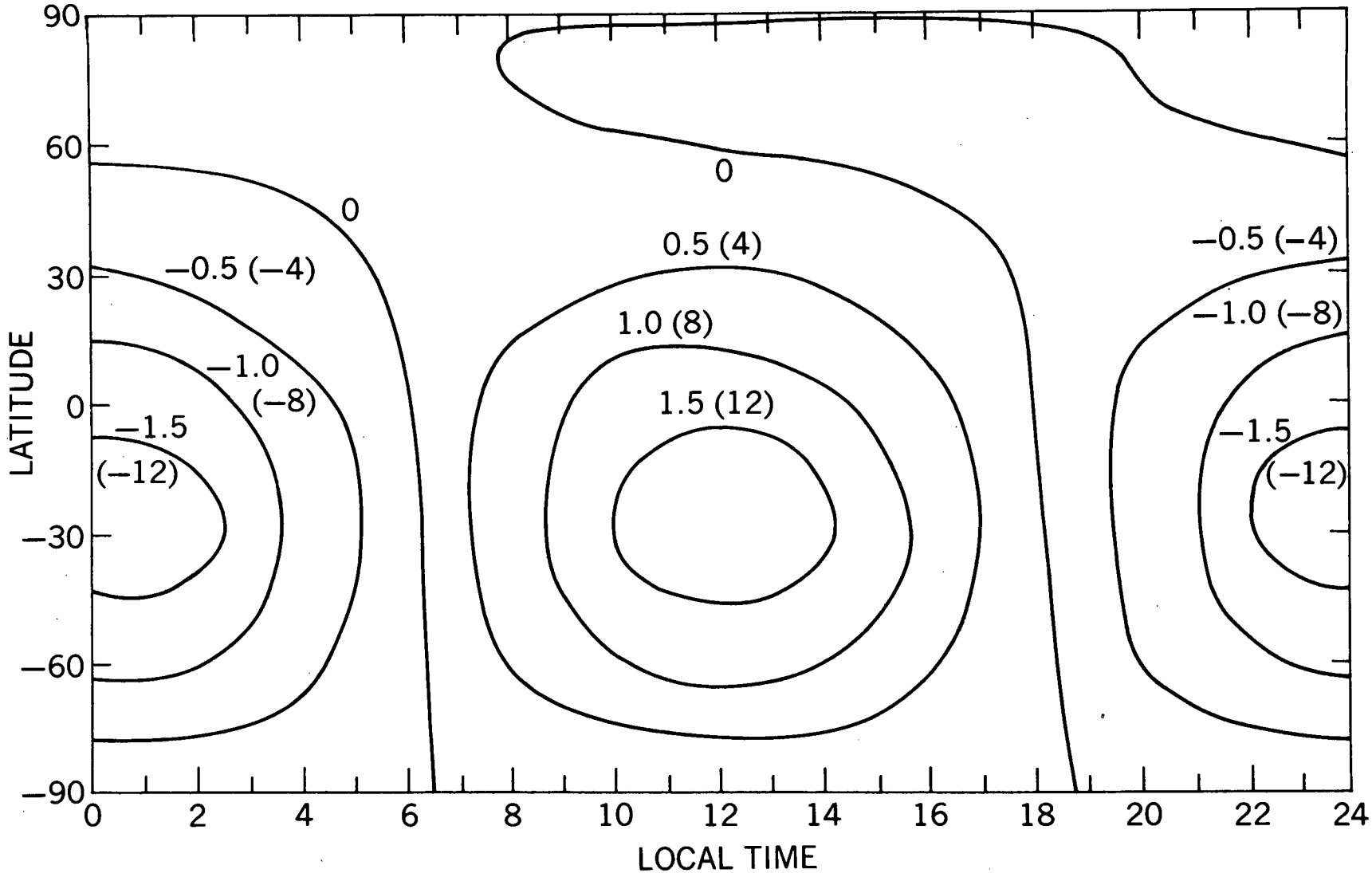


Figure 13. Total heating in an atmospheric column. The maximum heating is at the subsolar point and the total heating appears to be direct solar heating. The deviation in the north polar region is due to dynamics. The heating is expressed in ergs/cm$^2$/sec $\times$ 10$^{-5}$ and degrees K per day in parentheses.

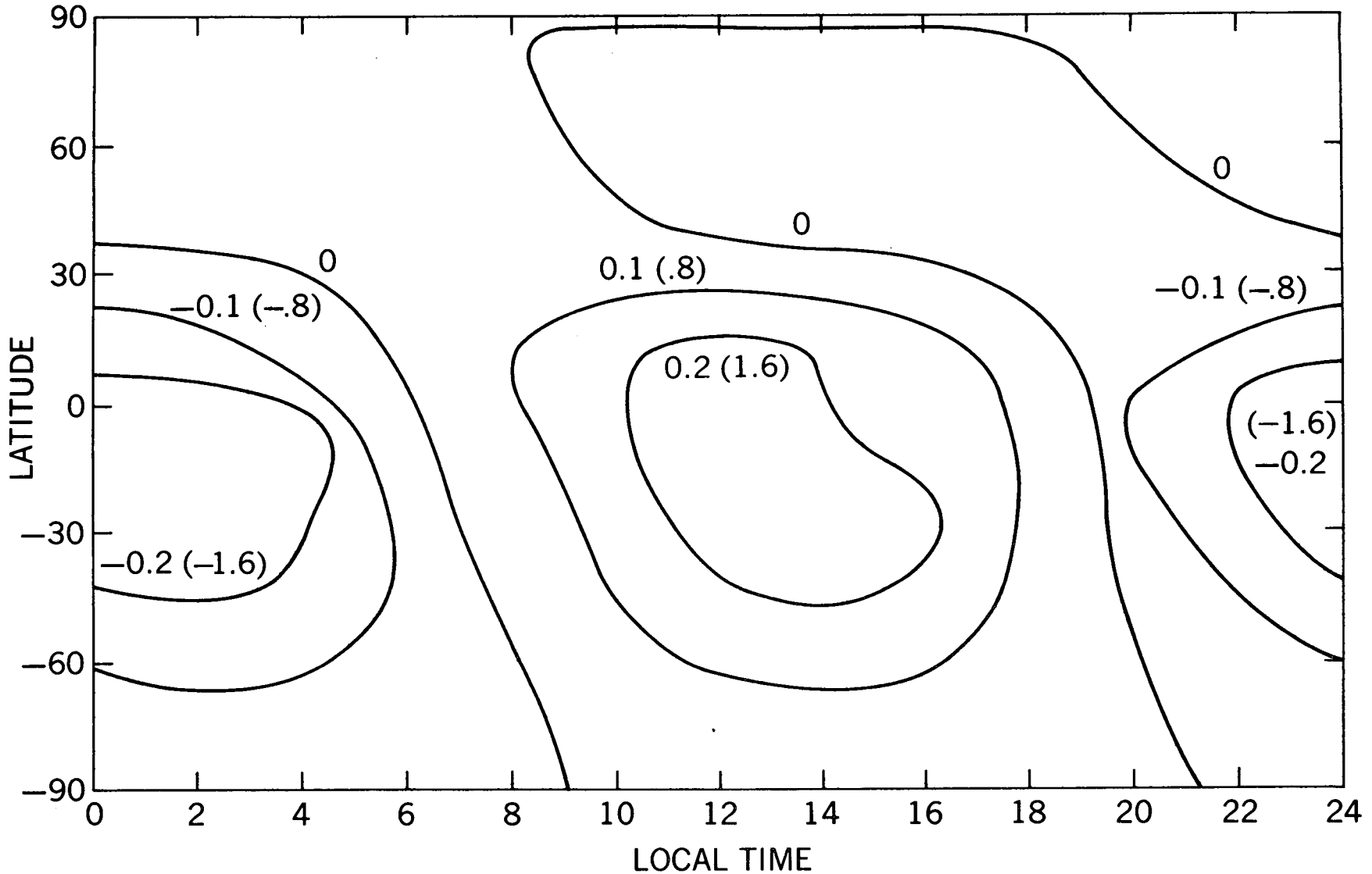


Figure 14. Heating due to the vertical motion of the atmosphere. This is in phase with the solar heating and is roughly 20% of the total. The heating is expressed in ergs/cm$^2$/sec $\times 10^{-5}$ and degrees K per day in parentheses.

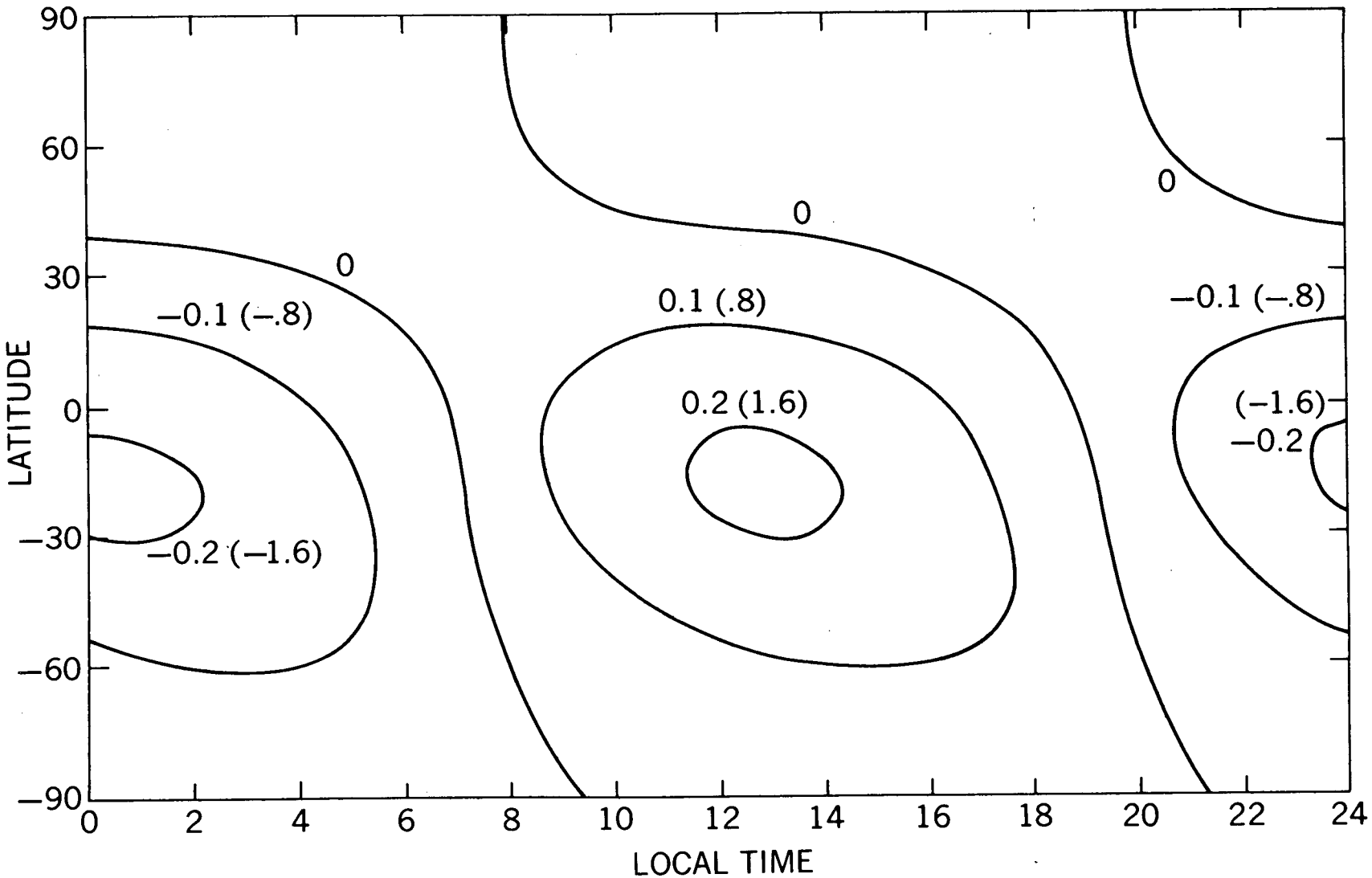


Figure 15. Heating due to the surface pressure. This is in phase with the solar heating and is roughly 10% of the total heating. The heating is expressed in ergs/cm$^2$/sec $\times 10^{-5}$ and degrees K per day in parentheses.